



UNIVERSITAT
POLITÈCNICA
DE VALÈNCIA



ESCUELA TÉCNICA
SUPERIOR INGENIEROS
INDUSTRIALES VALENCIA

CHEMICAL ENGINEERING MASTER THESIS

SIMULATION STUDY OF THE INTEGRATION OF HYDROGEN FUEL CELLS INTO UNMANNED AERIAL VEHICLES (UAV) AND ESTIMATION OF THE EMISSION SAVINGS ACHIEVED WHEN COMPARED TO A UAV WITH A GASOLINE COMBUSTION ENGINE

AUTHOR: IONA MCNAIR

SUPERVISOR: ALVARO MONTERO

SUPERVISOR: EDWARD BRIGHTMAN

Academic year: 2021-22

THANKS

I would like to offer special thanks to Prof. Alvaro Montero of the UPV Applied Thermodynamics Department, who shared his extensive knowledge on the subject and provided invaluable support for the duration of the project. He continually provided motivation, guidance and encouragement, ensuring that the project could be completed to its fullest potential. His patience and encouragement throughout the project has been invaluable and his enthusiasm for the project made me greatly appreciate working and learning about the subject. He was extremely willing to get involved in discussions to help develop my understanding and did not hesitate to offer help to aid the success of the project.

I would also like to thank Carlos Sanchez Diaz of the University institute for research in energy engineering, who proved to be a crucial contact in obtaining essential data for the progression of the project. He offered considerable wisdom and insight on the subject, and I am grateful for his help during my time in Valencia. Further, I would like to thank the drone manufacturing company *Quaternium*, as their data was vital for the successful completion of the project.

I would like to thank my academic supervisor Dr Edward Brightman, for his oversight the project and his support throughout the duration.

I would also like to extend my thanks towards the University of Strathclyde for giving me access to such great opportunities and enabling my degree, in particular the department of Chemical & Process Engineering. The department have given me the opportunity to carry out my study abroad, an experience which will remain with me for years to come.

Finally, I would like to thank my family and friends for all their support over the last five years, without it my university career would have been entirely different.

RESUMEN

En la actualidad existe una creciente preocupación por el medio ambiente y, en particular, por el consumo excesivo de combustibles fósiles tanto en el sector del transporte como en la generación de electricidad a través de centrales eléctricas tradicionales. Debido a esta preocupación, existe la necesidad de avanzar globalmente hacia una forma de vida más sostenible y respetuosa con el medio ambiente.

La opción de la tecnología del hidrógeno y su uso para las pilas de combustible se considera un recurso importante en el camino hacia una sociedad más sostenible. Su uso tiene el potencial de reducir las emisiones contaminantes y de gases de efecto invernadero que contribuyen al calentamiento global.

El objetivo del trabajo de fin de máster es estudiar y estimar el ahorro de emisiones que se podría conseguir en caso de sustitución de los motores de combustión de gasolina por pilas de combustible de hidrógeno para su uso en sistemas aéreos no tripulados.

La estrategia consiste en utilizar los datos actualmente disponibles para UAS de motores de combustión comerciales para compararlos con los disponibles a partir de un enfoque de simulación que estima las emisiones que se producen a partir del uso de una pila de combustible de hidrógeno. También se realizará un estudio de la autonomía conseguida por ambas tecnologías.

Palabras clave: Hidrógeno; Pila de combustible; PEMFC; sistema eléctrico híbrido; sistema de combustión híbrido; UAV; gases de invernadero; emisiones contaminantes.

RESUM

En l'actualitat existeix una creixent preocupació pel medi ambient i, en particular, pel consum excessiu de combustibles fòssils tant en el sector del transport com en la generació d'electricitat a través de centrals elèctriques tradicionals. A causa d'aquesta preocupació, existeix la necessitat d'avançar globalment cap a una forma de vida més sostenible i respectuosa amb el medi ambient.

L'opció de la tecnologia de l'hidrogen i el seu ús per a les piles de combustible es considera un recurs important en el camí cap a una societat més sostenible. El seu ús té el potencial de reduir les emissions contaminants i de gasos d'efecte d'hivernacle que contribueixen al calfament global.

L'objectiu del treball de fi de màster és estudiar i estimar l'estalvi d'emissions que es podria aconseguir en cas de substitució dels motors de combustió de gasolina per piles de combustible d'hidrogen per al seu ús en sistemes aeris no tripulats.

L'estratègia consisteix a utilitzar les dades actualment disponibles per a *UAS de motors de combustió comercials per a comparar-los amb els disponibles a partir d'un enfocament de simulació que estima les emissions que es produeixen a partir de l'ús d'una pila de combustible d'hidrogen. També es realitzarà un estudi de l'autonomia aconseguida per totes dues tecnologies.

Paraules clau: Hidrogen; Pila de combustible; *PEMFC; sistema elèctric híbrid; sistema de combustió híbrid; *UAV; gasos d'hivernacle; emissions contaminants.

ABSTRACT

At present, there is increasing concern for the environment, and in particular the excessive consumption of fossil fuels in both the transport sector and the generation of electricity through traditional power plants. Due to this concern, there is a requirement to globally move towards a more sustainable and environmentally friendly way of life.

The option of hydrogen technology and its use for fuel cells is considered to be a major resource in the move towards a more sustainable society. Its use has the potential to reduce polluting emissions and greenhouse gases which contribute to global warming.

The aim of the master's thesis is to study and estimate the emissions savings which could be achieved should gasoline combustion engines be replaced by hydrogen fuel cells for use in unmanned aerial systems.

The strategy is to use data currently available for commercial combustion engine UAS to be compared with that available from a simulation approach which suggests the emissions which are produced from the use of a hydrogen fuel cell. A study of the autonomy achieved by both technologies will also be carried out.

Keywords: Hydrogen; Fuel cell stack; PEMFC; Hybrid electric system; Hybrid combustion system; UAV; greenhouse gases; polluting emissions.

GENERAL INDEX OF THE FINAL MASTER'S PROJECT

- **Memory**
- **Budget**
- **Annexes**



UNIVERSITAT
POLITÈCNICA
DE VALÈNCIA



ESCUELA TÉCNICA
SUPERIOR INGENIEROS
INDUSTRIALES VALENCIA

MEMORY

**SIMULATION STUDY OF THE INTEGRATION OF
HYDROGEN FUEL CELLS INTO UNMANNED AERIAL
VEHICLES (UAV) AND ESTIMATION OF THE EMISSION
SAVINGS ACHIEVED WHEN COMPARED TO A UAV
WITH A COMBUSTION ENGINE**

MEMORY INDEX

Contents

1 MOTIVATION, JUSTIFICATION AND OBJECTIVES	1
1.1. Academic Justification.....	2
1.2. Professional Justification	2
1.3. Objectives	3
2 INTRODUCTION.....	4
3 RELEVANT LITERATURE INFORMATION	5
3.1 Comparison of Technologies.....	5
3.2 Conceptual Design of Fuel Cell-Battery Hybrid Drone	5
3.3 Conceptual Design of Combustion Engine-Battery Hybrid Drone	6
3.4 Commercially Available Designs	7
3.5 Batteries.....	8
3.6 DC/DC Power Converter.....	8
3.7 Internal Combustion Engines	9
3.7.1 Two-Stroke Engine Operation.....	9
3.8 Hydrogen Fuel Cells.....	10
3.8.1 Electrochemical Thermodynamics.....	11
3.8.2 Electrode Potential in a PEMFC.....	11
3.8.3 Electrochemical Kinetics	12
3.8.4 Electrochemical Half-Cell Reactions.....	13
3.8.4.2 Oxygen Reduction Reaction (ORR).....	14
4 METHODOLOGY.....	15
4.1 PEMFC Theoretical Efficiency.....	15
4.2 Hydrogen Consumption	16
4.3 Combustion Engine Efficiency	17
4.4 Emissions Produced.....	17
4.4.1 Emissions Produced during Operation	17
4.4.2 Emissions Produced through Fuel Production.....	18
4.5 Autonomy of Both Designs.....	18
5 RESULTS AND DISCUSSION	20
5.1 Fuel Consumption	20

5.2	Drone Efficiencies	20
5.2.1	Fuel Cell Efficiency	20
5.2.2	Combustion Engine Efficiency	21
5.3	Emissions Production	22
5.3.1	Emissions Produced during Operation	22
5.3.2	Emissions Produced through Fuel Production	23
5.3.3	Comparison of Overall Emissions	24
5.4	Comparison of Flight Autonomy	25
5.4.1	Fuel Cell Hybrid Demand Curve	25
5.4.2	Combustion Engine Hybrid Fuel Cell	27
5.5	Battery Specifications	28
5.6	Areas of Difficulty	29
5.7	Future Work Opportunities	29
6	CONCLUSIONS/OUTCOME	31
7	REFLECTION AND REVIEW	32
8	BIBLIOGRAPHY	33

FIGURES INDEX

<i>Figure 1- Representative diagram of the 'fuel cell-battery' hybrid system</i>	<i>6</i>
<i>Figure 2- Representative diagram of 'combustion engine-battery' hybrid system</i>	<i>6</i>
<i>Figure 3- 2 stroke engine representative diagram (10)</i>	<i>9</i>
<i>Figure 4- Polymeric electrolyte membrane fuel cell structure (4).....</i>	<i>10</i>
<i>Figure 5- Polarisation curve characteristics (5)</i>	<i>12</i>
<i>Figure 6- Intersection point between electrode and cathode</i>	<i>13</i>
<i>Figure 7- Activation energy for electrochemical half-cell reaction (16).....</i>	<i>14</i>
<i>Figure 8- Drone measurement specifications (5).....</i>	<i>22</i>
<i>Figure 9- Emissions produced through hydrogen production methods (21,22).....</i>	<i>23</i>
<i>Figure 10- Emissions produced by country's grid electricity (26).....</i>	<i>24</i>
<i>Figure 11- Comparison of emissions produced by each production method.....</i>	<i>24</i>
<i>Figure 12- Demand curve for fuel cell-battery hybrid.....</i>	<i>26</i>
<i>Figure 13- Modelling of hybrid system 'PEMFC + LiPo'</i>	<i>26</i>
<i>Figure 14- Demand curve for internal combustion engine-battery hybrid.....</i>	<i>27</i>
<i>Figure 15- Modelling of the hybrid system 'ICE + LiPo'</i>	<i>28</i>
<i>Figure 16- Grotthuss proton hopping mechanism (31)</i>	<i>1</i>
<i>Figure 17- Bipolar plates configurations.....</i>	<i>2</i>
<i>Figure 18- Structure of membrane electrodes (36).....</i>	<i>2</i>
<i>Figure 19- Influence of temperature on electrode potential (38).....</i>	<i>5</i>

TABLE INDEX

<i>Table 1- Technical specifications of the Hybrix 2.1 drone (Quaternium) (5)</i>	<i>7</i>
<i>Table 2- Technical specifications of the hybrid drone Hycopter (HES Energy Systems) (6)</i>	<i>8</i>
<i>Table 3- Hydrogen fuel cell characteristics (12,13).....</i>	<i>10</i>
<i>Table 4- Volumetric flow of hydrogen consumption under storage conditions</i>	<i>20</i>
<i>Table 5- Fuel cell energy conversion efficiency.....</i>	<i>21</i>
<i>Table 6- Combustion engine-battery hybrid efficiency.....</i>	<i>22</i>
<i>Table 7- Emissions produced during operation of combustion engine-battery hybrid drone ..</i>	<i>23</i>
<i>Table 8- Battery Specifications.....</i>	<i>29</i>
<i>Table 9- Enthalpy of formation under standard conditions for electrochemical oxidation reaction.....</i>	<i>11</i>
<i>Table 10- Entropy values for electrochemical oxidation reaction</i>	<i>11</i>
<i>Table 11- Hybrix 2.1 data provided by Quaternium</i>	<i>16</i>

1 MOTIVATION, JUSTIFICATION AND OBJECTIVES

Sustainable development is becoming a key driver in many industrial processes with a particular focus on the concept of circular economy. A significant feature of this circular economy is the reduction of finite fuels used for the transportation sector. The use of these fuels has been highlighted as a major source of harmful greenhouse gas emissions, with the use of fossil fuels being the primary contributor of carbon dioxide (CO₂) release (US EPA 2016). Hence, the development of alternative fuel sources is crucial for the planet and wider society. Utilising a more sustainable and environmentally friendly fuel would help reduce the global release of harmful greenhouse gases.

The growth of industry and technological advancements have led to an increase in energy requirements worldwide. UAVs, perhaps more commonly referred to as drones, have the potential to unlock new opportunities and generate greater efficiencies in industries and throughout society. These have many practical applications such as monitoring crowds, inspecting infrastructure, agriculture management and allowing access to remote areas which are difficult to reach (Anon n.d.).

This Master's Final Project will discuss the findings of UAV research that was carried out in the UPV Applied Thermodynamics department. The background information on these systems will discuss the key challenges faced by sole battery powered drones and highlight the necessity of hybrid systems. This section will also discuss the hybrid systems available, and theory required to understand these. The core of the report will outline the data accumulation and methods used, with this being followed by a discussion and conclusion of the results obtained. Further details can be found in the appendices and references provided at the end of the report.

The overall goal of the project is to gain an insight into the UAV industry and understand the influence which different power sources have on both the environmental impact of these and the available flight time. This work will provide key information to the department on the emissions produced by each drone power source and display the net emission savings which could be achieved by implementing one power over the other.

1.1. Academic Justification

This Master's Final Project aims to confirm that the student has acquired the knowledge and skills expected in their degree. In addition, it will fulfil the requirements set out to obtain 12 ECTS credits necessary to complete the Master's degree project at the Polytechnic University of Valencia.

1.2. Professional Justification

From a professional perspective, the development of drone technology has the potential to significantly reduce the carbon dioxide emissions generated by the transport sector. This reduction could make a major impact on the decrease of global warming, and as a result aid with the move toward a more sustainable future.

In particular, the analysis of the different hybrid drone systems to help further the development of the technology is necessary. Hybrid systems analysed include those composed of a fuel cell and battery, and of an internal combustion engine and battery as these are identified as those with the most potential for future implementation. Once the analysis of the hybrid systems has been conducted, and a comparison of both the flight autonomy and emission production has been achieved, the next phase of the development process would be to proceed with experimental trials and flight tests with commercial models with adjustments which have the potential to improve these factors for both systems.

Finally, if results obtained from the flights were to be satisfactory, and the adjustments feasible to integrate into the systems, a demonstration of the real energy potential of the hybrid technology could be displayed. This could be a boost for the development and application of hybrid drone systems within the transport industry, particularly that for delivering goods.

1.3. Objectives

The main object of this project was to carry out a fair and extensive comparison of two different drone hybrid systems, and make an estimation on the net emission savings which could be made should one hybrid power source be replaced by the other. Currently, the industry-leading commercial drone models are those which utilise lithium-ion polymer (Lithium-Polymer, LiPo) batteries only as the power source, mainly due to their high energy density as well as low size and weight.

However, LiPo batteries require very high discharge rates to be able to supply the demand of energy of the drones electric current intensity, which favours the discharging of the battery and limits the available flight time of the drone greatly.

To combat this, an analysis and comparison of two hybrid drone systems with great potential for further technology advancements and industrial implementation. However, when compared to the battery only powered drones the two hybrid systems are heavier. This justifies their application for emergency situations as they can carry large payloads, such as emergency search and rescue situations.

This Master's Project proposes to estimate the net emission savings which could be made should a fuel cell take the place of an internal combustion engine within a hybrid system. In addition to this, a comparison of the available flight times of both systems is carried out to assess areas which need improvement in the future. To achieve this, the following aims were outlined:

1. Estimate the emissions produced by hydrogen fuel cells and internal combustion engines.
2. Determine the power and intensity requirements for the drone over an hour-long operation period.
3. Compare the two hybrid drone systems on both points, and assess the different factors which could impact the results of this.

Personal aims upon completion of the project:

1. Further knowledge on UAVs and the challenges faced by the industry.
2. Gain experience working as part of a professional project, using data analysis, and taking theoretical knowledge to apply to a real-life scenario.
3. Demonstrate the ability to learn independently, problem solve, manage a project plan, and overcome communication and language barriers.

2 INTRODUCTION

In recent years, the energy demand worldwide has increased due to population growth and significant industrial development. This has led to an unsustainable situation with excessive consumption of fuel, particularly in the transport sector.

As is well known, the world is currently facing serious environmental problems in relation to greenhouse gas emissions which lead to global warming. A large amount of these emissions are caused by the use of fossil fuels, and the overexploitation of these has generated an uncertainty in the area regarding the supply due to their finite existence. The transport sector has the largest consumption of these fossil fuels, and thus development of a new sustainable energy source is required as a solution to reduce greenhouse gas generation.

In this sense, drones have recently emerged as a delivery method that could be used in place of certain delivery vehicles currently in place. Drone technology most used currently is that which utilises batteries only, thus eliminating the polluting emissions which are generated by the combustion of fossil fuels. However, these have low energy density and so cannot travel long distances without requiring recharging, and so a model with more energy availability is required in order to integrate drone technology further.

This introduces the idea of hybrid drones, which overcome the energy availability issues but still allow for the implementation of the battery fast response characteristic. The two current hybrid drone models with the most potential are one which implements an internal combustion engine with the battery, and another which uses a hydrogen fuel cell with the battery.

A comparison of these two drones should be conducted in order to assess which design is stronger in certain categories. It was concluded that for the purpose of this Master's Project, the emissions produced would be compared, as well as the drone flight autonomy.

3 RELEVANT LITERATURE INFORMATION

Due to the nature of the project being data analysis, it is imperative that literature sources used be selected carefully and that a range of data be analysed for accuracy. As much data which was focused on the fuel cell hybrid was obtained from simulation and test flight carried out before commencement of the project by the university this data is accurate and reliable. A significant amount of the data obtained for the combustion engine drone was provided by a company named *Quaternium*, who sent drone specifications for multiple payloads, meaning this information can also be deduced as reliable.

3.1 Comparison of Technologies

An effective UAV system must balance two opposing requirements: the need for sustained power production (energy capacity) to achieve flight endurance, and the demand for peak load levelling to achieve acceptable in-flight dynamic performance. For this reason, hybrid systems where the battery is the primary power source do not have the long flight time availability that those where it is the secondary power source have. Purely electrical propulsion, found in UAVs which utilise a battery for energy storage and power production, have the advantages of fast load response time, hence battery energy storage should be retained within the hybrid system (Krznar and Piljek 2021). However, batteries do not possess as great an energy density as the fuel cell and internal combustion engine, meaning for longer flight time the battery size would have to increase significantly. The availability of energy on-board for solely battery powered drones is therefore lower than that of hybrid systems, meaning the flight time without the requirement of recharging is significantly lower.

3.2 Conceptual Design of Fuel Cell-Battery Hybrid Drone

The selected technology for the hybrid system incorporates a proton exchange membrane (PEM) as a solid electrolyte. This offers a low operating temperature, fast system response against the electrical current demand and allows the use of hydrogen fuel. An open cathodic configuration is proposed to take advantage of the atmospheric air to act as an oxidizing agent as well as a cooling fluid for the system.

The battery is necessary to start the drone operation and must meet the balance demand of the system during the switching on and off phases of the vehicle's starting and stopping elements. Due to the recharging capability of the battery, the dimensioning was carried out to slightly exceed the average consumption of the drone to allow for battery recharging. Thus, the size of the battery is minimised, but sufficient energy capacity must be ensured to allow the hybrid system to reach the consumption peaks of the drone during take-off and landing.

To adapt the voltage produced by the PEMFC to that from the battery, a DC/DC power converter is required. So, management of the electrical energy produced by this system is carried out by controlling the electrical current generated by the fuel cell powered stage to the power peaks of the drone flight system.

The magnitude of current generated by the PEMFC during the stationary flight phases should marginally exceed the average consumption, to both allocate part of the electric current for the battery recharging process and meet the balance requirements of the drone and keep the flight systems of the vehicle in operation.

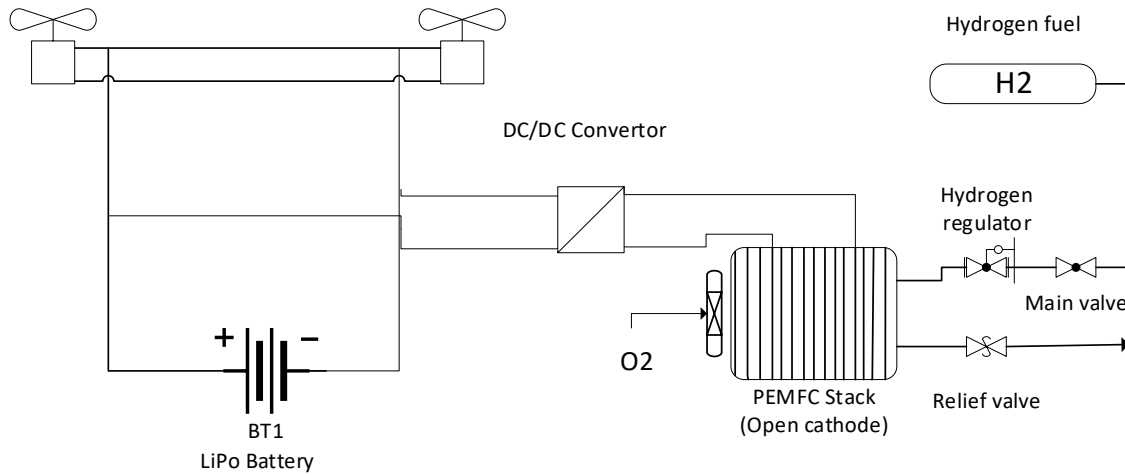


Figure 1- Representative diagram of the 'fuel cell-battery' hybrid system

3.3 Conceptual Design of Combustion Engine-Battery Hybrid Drone

A combustion engine-battery hybrid system incorporates an internal combustion engine (ICE) and electricity generator (EG). This hybrid drone supplies the bulk of energy to the common DC bus (power distribution system) via an appropriate AC to DC rectifier, which maintains the DC bus operating voltage level. The battery represents an auxiliary power source, connected in parallel to the DC bus, and is primarily used for peak load shaving (where the battery proactively manages the overall drone demand to eliminate short-term demand spikes which set a higher peak), and load levelling at very high hybrid power-train loads (Krznar and Piljek 2021).

The main advantage of such a hybrid system is that it can support the DC bus voltage under highly dynamic loading conditions, and as a result is able to fully utilise the fast response ability of the propellers electric motor drives, an essential requirement for a high-quality performance of the overall flight control system.

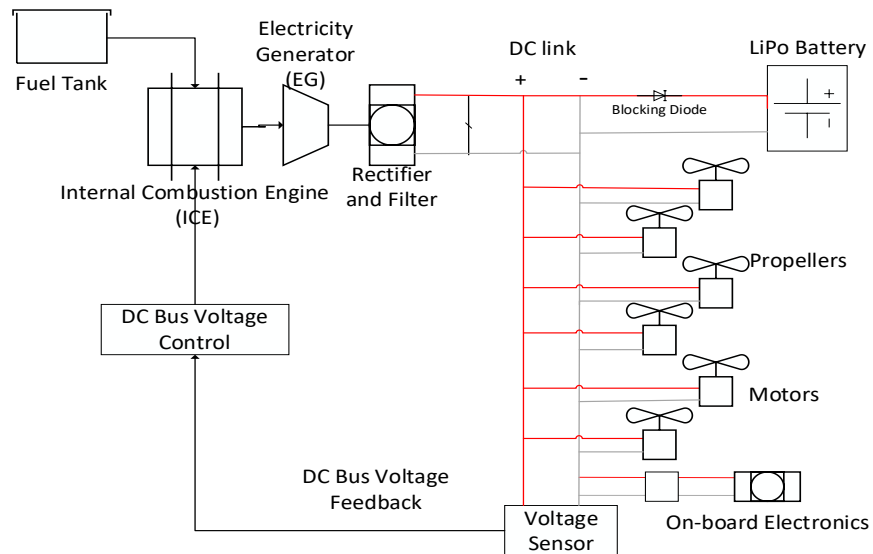


Figure 2- Representative diagram of 'combustion engine-battery' hybrid system

Figure 2 demonstrates the hybrid power system with the internal combustion engine being directly connected to the electricity generator, this supplies power via a three-phase full-wave diode rectifier and is controlled completely by the engine throttle command.

3.4 Commercially Available Designs

Drones offer great versatility and can be of particular importance to emergency situations where they are able to carry out rescue tasks including the transport of medical supplies, clean water, and aerial land inspection.

Drones are often developed for specific sectors. *Hybrix 2.1* is an example of a commercial model developed by *Quaternium* which can be utilised in emergency situations such as those where remote areas must be reached.

The *Hybrix 2.1* offers a hybrid system which merges electricity provided by a set of batteries with an internal combustion engine. The hybrid technology overcomes certain limitations evident in the drone market with regards to autonomy, allowing for search and rescue of people both on land and sea.

Table 1- Technical specifications of the *Hybrix 2.1* drone (Quaternium 2021)



Quaternium	
Maximum Weight (MTOW)	20//25 kg
Empty Weight	13 kg
Maximum Load	5//10 kg
Flight Time (with maximum load)	2 hours
Flight Time (with no load)	4 hours
Maximum Speed	80 km/hour


Here, the primary power source is the internal combustion engine. The electrical LiPo batteries keep the electronic components of the drone working (cameras, GPA...), whilst the combustion engine nourishes a generator connected to the 4 electric motors that drive the drone's flight rotors (Anon n.d.).


To reduce emissions which contribute to greenhouse gases produced through fossil fuel combustion, as well as achieving better flight autonomy than that from purely electrical power supply via batteries, a different power source must be developed. This introduces a new hybrid system which improves drone flight time and solves battery limitations by utilising fuel cells.

One technology which offers an electric hybrid system formed by a PEMFC and LiPo battery is the *Hycopter* model by Asian company *Hydrogen Energy Systems (HES)*. This is a long endurance drone which can reach up to 3.5 hours of continuous flight without the need to stop for cylinder replacement storage for hydrogen fuel or battery recharging.

The main electrical power source of this technology is an open cathode fuel cell, designed to take advantage of atmospheric air as an oxidising agent and as coolant fluid in the electrochemical device. The power system is made up of an ultra-light and compact air-cooled PEM fuel cell from the *Aerostak* series.

Table 2- Technical specifications of the hybrid drone Hycopter (HES Energy Systems)



	
Maximum Weight (MTOW)	16.5 kg
Empty Weight	14 kg
Maximum Load	2.5 kg
Tank Capacity	5 – 9 – 12 L
Flight Time (with maximum load)	90 minutes
Flight Time (with no load)	3.5+ hours
Maximum Speed	48 km/hour

For this design, the PEMFC can be attached to different sized storage cylinders of highly pressurised hydrogen, made from carbon fibre to both be strong and as light as possible.

One beneficial feature of the *Aerostak* series PEMFC's is the option of incorporating the electronic components necessary to form hybridisation with a LiPo battery. The drone uses a LiPo battery to generate additional electrical power when the energy demand exceeds that of the maximum power available from the PEMFC and allows the battery to be recharged when there is an electrical surplus in the system.

3.5 Batteries

The battery is an essential component as it starts operation and must comply with the demand of the drone. The battery supplies the balance of the system of the electrical and electronic components which initiates the start-up of the drone's flight. In addition, the battery allows the electrical consumption of the drone to be achieved during take-off and landing which are the most energy-intensive phases of flight.

Most commonly, a Lithium-ion polymer battery (Lithium-Polymer, LiPo) is utilised. This is mainly due to the high energy density offered as well as being compact in size and lightweight (Grepow 2020).

3.6 DC/DC Power Converter

To adapt the voltage provided by the power source to the voltage of the LiPo battery of the hybrid system, a DC/DC power converter is required. This DC/DC converter has a step-down configuration as the number of cells selected for battery sizing is limited by the voltage- meaning that the primary power source voltage should always be higher than that of the LiPo battery (Krznar and Piljek 2021).

3.7 Internal Combustion Engines

The figuration utilised for this project combines an internal combustion engine coupled with an electricity generator as a propulsion system. An internal combustion engine is a machine which converts internal energy into mechanical energy through the combustion of fuel (Anon n.d.).

The ICE is directly connected to the EG shaft which supplies the common DC bus through a diode rectifier, thus acting as the DC power supply, controlled by the engine throttle command. A LiPo battery with suitable charge capacity and a terminal voltage range matching the DC bus voltage target is connected to the common DC bus through a blocking diode to prevent uncontrolled battery charging from the DC bus, and related battery current and voltage overloads (Krznar and Piljek 2021; Townsend et al. 2020).

When the DC bus voltage is lowered below the battery terminal voltage due to ICE-EG set slow dynamics in covering sudden DC bus load change, the blocking diode can change to be forward biased. This allows the battery to be discharged and supply the DC bus with the additional requirements. To facilitate the ICE-EG set taking over after the initial DC bus voltage drop, the DC bus voltage control system is based on the ICG-EG set throttle command equipped with the appropriate voltage controller. This means the ICE mechanical load can be matched by the load from the EG.

3.7.1 Two-Stroke Engine Operation

The engine used by *Quaternium* is described as 2-stroke. This type of combustion engine completes one power cycle with two strokes (up and down movements) of the piston. *Figure 3* illustrates the sequential strokes which equate to one full power cycle, highlighting key elements of the engine. The actions of both intake and exhaust occur between the compression and power strokes. The power stroke occurs after the spark plug has fired, the air/fuel mixture has been ignited, and an immediate flame front has been created. The chemical energy of the burning air/fuel mixture creates heat and pressure which force the piston down the cylinder. This chemical energy is converted into mechanical energy both by the piston and the connecting rod to rotate the engine crankshaft (Anon n.d.).

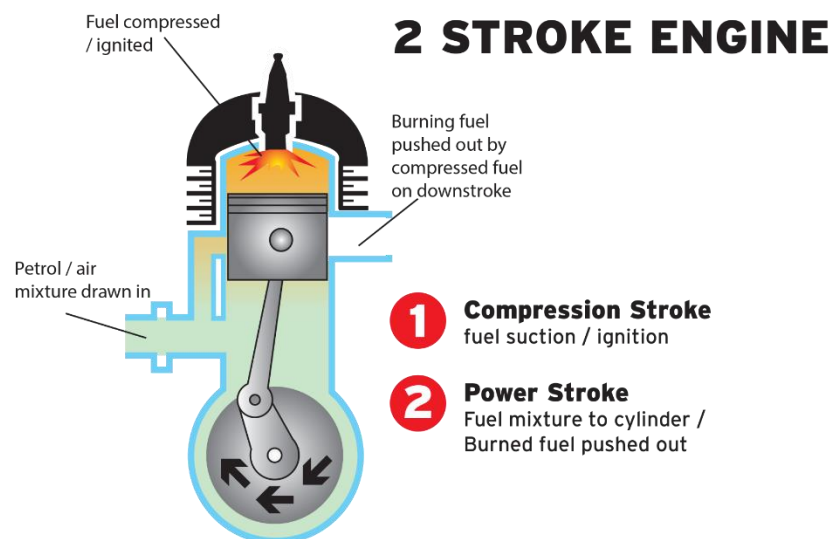


Figure 3- 2 stroke engine representative diagram (Anon n.d.)

The generator is then used to convert the mechanical energy into electrical energy. This is done by capturing the power of motion and turning it into electrical energy by forcing electrons of the combustion

reaction products onto the blades to rotate the rotor shaft. This then converts the mechanical, or kinetic, energy of the rotor to electrical energy (US Energy Information Administration (EIA)).

3.8 Hydrogen Fuel Cells

Fuel cell technology is at the forefront of the developing transport sector, offering a clean and sustainable alternative to fossil fuel powered vehicles. It has the potential application for any type of system which requires the supply of electrical energy and so can be applied to many electrical or electronic devices.

Each fuel cell configuration has specific operating characteristics which are dependent on the technology used. The characteristics of the hydrogen fuel cell used as the primary power source for the hybrid drone can be seen in Table 3 below.

Table 3- Hydrogen fuel cell characteristics (Brightman 2021; Rosli et al. 2017)

Characteristic	PEMFC
Fuel	Hydrogen (H ₂)
Oxidizing agent	Air (O ₂)
Electrolyte	Solid polymer cation exchange membrane
Nature	Acid
Temperature Range (°C)	20 – 100
Anodic Reaction (Hydrogen)	
Cathodic Reaction (Oxygen Reduction Reaction)	$O_2 + 4H^+ + 4e^- \rightarrow 2H_2O$
Carrier Ionic Charge	Protons (H ⁺)
Conversion Efficiency (%)	50-60
Power (kW)	10-250
Applications	Auxiliary generator, transport

Fuel cells embody a series sequence of various single cell units, generating a stack of fuel cells to obtain a desired voltage and electrical power. The elementary fuel cell design is formed by the following basic components:

- A proton exchange membrane as an electrolyte
- The anode, cathode and electrode which are covered with a catalyst
- Gas diffusion layer
- Bipolar plates which facilitate the diffusion of reactants and products

Figure 4 presents the PEMFC structure, displaying the inputs and outputs for each layer.

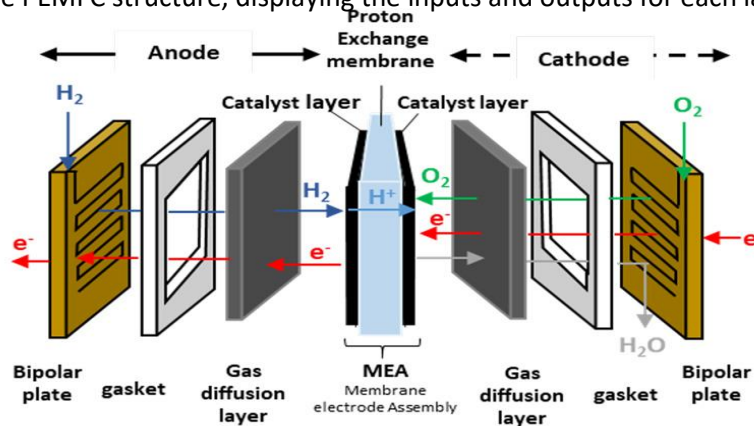


Figure 4- Polymeric electrolyte membrane fuel cell structure (GD-EOS)

The operation of a PEMFC-type fuel cell starts with the supply of reactants in their respective compartments. The channels present in the bipolar plates allow reactive gases to disperse homogeneously over the entire surface of the electrodes. The porous structure of the electrocatalyst leads to improvement in the kinetics of electrochemical half-reactions on the anode and cathode.

Through the oxidation half-reaction hydrogen is dissociated, resulting in protons passing through the polymeric membrane of the electrolyte. To enable the oxygen reduction half-cell reaction on the cathode, electrons run through the external electrical circuit. The water released here is utilised to maintain fuel cell conditions including appropriate wetting of the polymeric membrane and improvement of the ionic conductivity.

A discussion of the different components within a fuel cell, and the role they play in the successful operation can be found in *Appendix O*.

3.8.1 Electrochemical Thermodynamics

The applied thermodynamics in a polymer electrolyte membrane fuel cell focuses on energy transformation processes. The fuel cell can be considered to be an energy conversion device as the chemical energy stored in hydrogen fuel is transformed directly into electrical energy. Whether an electrochemical reaction is energetically spontaneous or not can be predicted by applying thermodynamic principles and equations. It is also possible to establish the maximum electrochemical conversion yield achievable in such devices (Khotseng 2019).

It should be noted that the real behaviour is almost certainly lower than the maximum limit set by thermodynamic principles. This is due to electrochemical kinetics, which allow for a more accurate prediction of the behaviour of a fuel cell and allow for a better understanding of the energy limitations of such systems. *Appendix O* expands further by using the first and second laws of thermodynamics to express the internal energy variation of the system.

3.8.2 Electrode Potential in a PEMFC

The capacity an electrochemical system has to produce electrical work is directly related to the electrode potential of a fuel cell (E) and is dependent on the amount of electrical charge created in the device due to electrochemical reactions. By considering the work potential of hydrogen fuel, an expression which relates the electrode potential to the Gibbs free energy can be obtained:

$$-\Delta G = n \cdot F a \cdot E \quad \text{Equation 2.1}$$

When considering the reaction under standard conditions it is possible to determine the reversible electrode potential for the overall electrochemical reaction:

$$E^0 = \frac{\Delta G^0}{n \cdot F} = \frac{237 \times 10^3 \left(\frac{J}{\text{mol } H_2} \right)}{2 \left(\frac{\text{mol } e^-}{\text{mol } H_2} \right) \cdot 96500 \left(\frac{C}{\text{mol } e^-} \right)} = 1.228 \text{ V} \quad \text{Equation 2.2}$$

From this result it is seen that under standard conditions, the maximum obtainable electrode potential for the $H_2 - O_2$ electrochemical system is approx. 1.23 V. It is therefore necessary to series stack various single fuel cells to achieve higher voltages in the electrochemical device.

However, operation of PEMFCs is done under non-standard conditions. According to characteristics specified in Table 3, fuel cells with proton exchange polymeric membranes operate in low temperature ranges (20 - 100°C) and pressures slightly above that of atmospheric (3-5 bar). The impact which both the pressure and temperature have on the fuel cell operation is presented in *Appendix O & O* respectively. In addition, there are concentration gradients of the reactive substances present on the surface of electrodes caused by overpotentials in the fuel cell.

3.8.3 Electrochemical Kinetics

The maximum achievable energy conversion performance in fuel cells is understood through thermodynamic principles. The thermodynamic cell potential represents the maximum voltage which can be obtained in a single fuel cell under certain operating conditions and in the absence of an electric current.

However, actual operation of fuel cells shows significant deviations from the situation laid out by theoretical thermodynamic limits (displayed in *Appendix O*). When the fuel cell begins to generate electrical current, the cell potential decreases due to the presence of irreversible losses in the electrochemical process. These arise due to a variety of situations such as species crossover through the electrolyte, internal current from electron leakage, contaminants etc. In practice, the polarisation curve represents the real operation of a fuel cell and allows the causes of progressive losses to be identified.

Figure 5 displays a characteristic polarisation curve for real operation of a fuel cell, here the presence of different types of polarisations can be observed according to the increase in current intensity generated by the electrochemical device, showing a progressive decrease in the generated cell voltage.

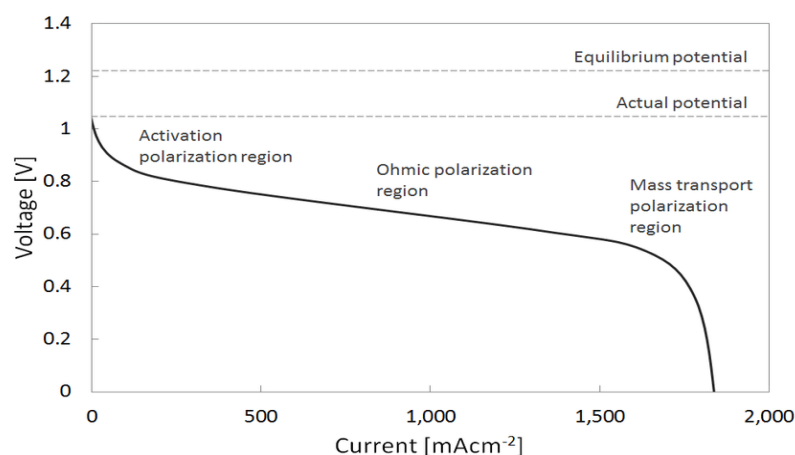


Figure 5- Polarisation curve characteristics (Valle 2015)

There are three types of polarisation which directly impact the cell voltage, where each source of loss is related to a different stage of the overall electrochemical conversion process (Brightman 2021).

- Activation polarisation: Occur at low currents due to an activation barrier which impedes the conversion of reactants to products. Associated with the electrochemical kinetics of the oxidation and reduction half-cell reactions. Limits the rate of conversion of reactants to products.

- Ohmic (IR) polarisation: As current increases, resistive voltage losses begin to prevail due to proton transport through the polymeric membrane (ionic resistance) and electronic transport by conductors (electronic resistance). Due to charge transfer processes obeying Ohm’s law, this is referred to as Ohmic losses.
- Concentration polarisation: Dominant at high currents where limitation is reached by the mass transfer of reagents and the electrolyte medium.

The actual cell voltage provided by the fuel cell (V) can be described by the thermodynamic cell potential (E_{OCV}) with consideration for the various voltage losses (overpotentials) taken.

$$V = E_{OCV} - \eta_{act} - \eta_{ohmic} - \eta_{conc} \quad \text{Equation 2.3}$$

3.8.4 Electrochemical Half-Cell Reactions

Any electrochemical reaction implies a transfer of electric charge without direct contact between the reactive species. The electrons generated by the oxidation reaction at the anode travel through an external conductive element until they reach the cathode to be consumed in the reduction reaction. This flow of generated free electrons represents an electrical current, allowing electrical work to be performed in fuel cells.

Therefore, both electrochemical reactions require the transfer of electrons between the electrode material and the reactive substance (reducing and oxidising). The process can be considered heterogeneous, as reactions can only take place on the interface between the electrode and electrolyte. In the PEMFC, hydrogen fuel acts as the reducing agent and undergoes oxidation at the anode electrode, whilst atmospheric oxygen is utilised as the oxidising agent which undergoes reduction at the cathode electrode.

3.8.4.1 Hydrogen Oxidation Reaction

The overall reaction can be seen below, with the exchange of electrons taking place on the surface of the electrode.



This is due to the hydrogen gas and protons being unable to exist within the electrolyte, and so the reaction between hydrogen, protons, and electrons must occur where the electrode and electrolyte intersect, shown in Figure 6- Intersection point between electrode and cathode.

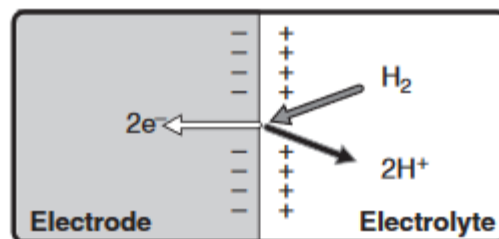
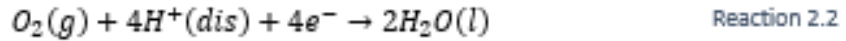


Figure 6- Intersection point between electrode and cathode

3.8.4.2 Oxygen Reduction Reaction (ORR)

The anodic oxygen reduction reaction is more complex than the cathodic reaction, with alternative pathways possible. The most likely possibility entails a platinum metal electrode as the catalyst in a direct 4-electron dissociative mechanism. As with the hydrogen oxidation reaction, the exchange of electrons takes place at the surface between the cathode and the electrolyte (Ma et al. 2019).



By considering the global reaction which takes place in a PEMFC where gaseous hydrogen is used as the fuel source and atmospheric oxygen as the oxidant, the cathodic half reaction (ORR) has slower electrochemical kinetics in relation to the anodic half reaction (HOR). This can be deduced directly by comparing the activation energy values for both electrochemical half-reactions in .

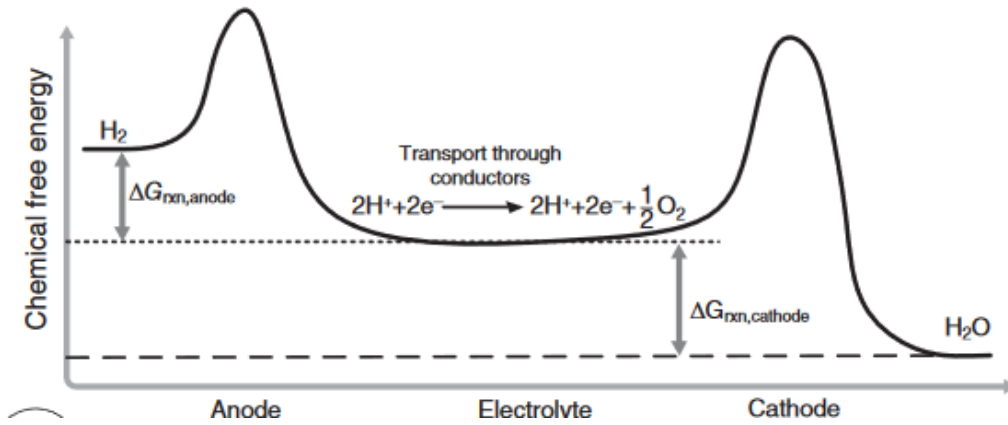


Figure 7- Activation energy for electrochemical half-cell reaction (O'Hayre et al. 2016)

It can be deduced that the oxygen reduction half-cell reaction at the cathode has a higher activation energy than that of the hydrogen oxidation half-cell reaction at the anode. The mechanisms for both reactions can be seen in *Appendix 0*, where the rate determining step for each is highlighted. This higher activation energy results in a larger quantity of electrocatalyst being required for the cathodic reaction in an attempt to reduce the activation barrier of the reduction reaction and improve overall electrochemical kinetics of the fuel cell (Matthey n.d.).

4 METHODOLOGY

The objective of the study is to complete a fair comparison of the emissions production and flight time availability of different hybrid drone systems. Data collected for the study was obtained using both simulation data and literature sources for real flights. The data taken from simulation was from a reliable source (collected by Polytechnic University of Valencia) prior to commencing this study. That taken to model the combustion engine drone was acquired primarily from the drone manufacturing company, *Quaternium*, shown in *Appendix 0*.

When modelling these drones, certain parameters were required for calculating fuel consumption, and so technical specifications of existing commercial models were consulted.

The maximum energy conversion efficiency represents the situation where the greatest useful power can be extracted from the drone power source.

To estimate the energy consumption of the combustion engine drone, an existing commercial drone was used to extend an analytical model, based on the conservation of momentum. This method was adopted from an article which discusses the energy use and life cycle emissions of drones (Stolaroff et al. 2018). The method is outlined in *Section 4.3*, with an extensive method displayed in *Appendix 0*. Energy used by the drone is dependent on speed of travel. This was estimated to be 14 m/s (50 km/h), the average cruise flight speed for a *Quaternium* drone (Anon n.d.).

The method laid out for the energy conversion efficiency for the fuel cell is developed using the Gibbs Free Energy expression. With knowledge of the enthalpy and entropy terms, it is possible to calculate the theoretical work potential of the PEMFC.

4.1 PEMFC Theoretical Efficiency

The theoretical efficiency of a hydrogen fuel cell was calculated to be 83% utilising the enthalpy of formation and entropy values for the oxidation reaction species. This calculation is displayed in *Appendix 0*, with the relevant data presented. However, PEM fuel cells are limited to energy conversion efficiencies around 50-60% (Table 3). This is due to polarisation, related to the kinetics of the fuel cell, where electrical power losses are produced which slightly reduce the efficiency of the energy conversion process.

The electrochemical kinetics cause electrical power losses which contribute to the reduction in efficiency of the energy conversion process should therefore be analysed.

Fuel cell behaviour is defined as a function of the output voltage (U_{cell}). This can be used to determine the theoretical energy efficiency of the drone whilst taking into consideration electrochemical kinetic losses. This can be determined from the thermodynamic cell potential and voltage losses due to polarisation. By establishing a minimum cell voltage ($U_{C_{min}}$) and maximum current density ($I_{C_{max}}$) value, the limiting current density is not reached and the operating region where the voltage losses expression due to concentration is avoided. This was done using simulation data, and therefore the following equation can be adopted for the output voltage:

$$U_{cell} = E - \eta_{act} - \eta_{ohmic} \quad \text{Equation 3.1}$$

Determination of the potential different (E) alongside the activation (η_{act}) and ohmic (η_{ohmic}) losses can be seen in *Appendix 0*.

Assuming the energy potential of hydrogen under standard conditions does not change substantially in the temperature range of 0-100°C and 0-100 bar, it is possible to determine the maximum cell potential

considering all the heat of reactions released is fully exploited to obtain useful electrical work from the system. This term is named thermoneutral voltage (U_{TH}), calculated as follows.

$$U_{TH} = \frac{Q_{max}^0}{n_e F a} = \frac{286 \times 10^3 \left(\frac{J}{mol H_2} \right)}{2 \left(\frac{mol e^-}{mol H_2} \right) \cdot 96485 \left(\frac{C}{mol e^-} \right)} = 1.482 V \quad \text{Equation 3.2}$$

The energy conversion efficiency (η_e) of the PEMFC can then be calculated.

$$\eta_e = \frac{U_{cell}}{U_{TH}} \quad \text{Equation 3.3}$$

The electrochemical device allows for generation of electricity in the form of direct current and has a high energy conversion efficiency, eliminating the power losses associated with the various intermediate transformation stages required by the thermal combustion process. Therefore, it should be seen from results that the efficiency for the combustion engine is lower than that for the fuel cell.

4.2 Hydrogen Consumption

The amount of hydrogen consumed during operation is necessary to determine the flight range of the drone alongside the emissions generated. The software TRNSYS, used for the simulation of the fuel cell hybrid, allowed for a time integration of the volumetric flow rate of hydrogen consumed to be simulated to obtain the total volume of hydrogen required in the storage tank. The flow of hydrogen consumption is expressed under standard conditions ($P_{H_2} = 1 \text{ atm}$; $T_{H_2} = 0^\circ\text{C} = 273\text{K}$). This allows the hydrogen consumption in storage tank conditions to be determined.

Knowing the volumetric flow of hydrogen consumed under standard conditions (Q_{H_2N}), the molar flow of hydrogen consumed (F_{H_2}) can be determined by utilising the ideal gas equation, and applying the hydrogen compressibility factor ($z=1$) (Makridis 2016).

$$F_{H_2} = \frac{P \cdot Q_{H_2N}}{z \cdot R \cdot T} \quad \text{Equation 3.4}$$

The storage conditions of hydrogen in relation to the pressure and temperature within the storage tank (P_{H_2st} ; T_{H_2st}) are applied to calculate the actual consumption of hydrogen fuel (Q_{H_2}). However, as the hydrogen in the storage tank is highly pressurised, the correction that implies the deviation from the ideal behaviour must be included by means of the hydrogen compressibility factor in the storage conditions of the fuel tank (z_{H_2}):

$$Q_{H_2} = \frac{z_{H_2} \cdot \dot{n}_{H_2} \cdot R \cdot T_{H_2}}{P_{H_2}} \quad \text{Equation 3.5}$$

Alternatively, the total moles of hydrogen consumed (n_{H_2}) can be obtained from the total volume of hydrogen required under normal conditions (V_{H_2}):

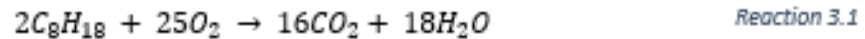
$$n_{H_2} = \frac{P \cdot V_{H_2}}{z_{H_2} \cdot R \cdot T} \quad \text{Equation 3.6}$$

Taking the hydrogen storage conditions, the actual volume of hydrogen fuel can be calculated using the ideal gas equation which has been corrected by the compressibility factor of hydrogen:

$$V_{H2} = \frac{z_{H2} \cdot n_{H2} \cdot R \cdot T_{H2}}{P_{H2}} \quad \text{Equation 3.7}$$

4.3 Combustion Engine Efficiency

Using the *Quaternium* design *Hybrix 2.1* as a basis for the combustion engine, the fuel used is a mixture named octane 95 oil. The combustion reaction can therefore be assumed to follow that displayed below (Li 2021).



This reaction assumes that the combustion is complete and does not produce any by products which differ from that shown above, such as unreacted oxygen. Data provided by *Quaternium* included that for the consumption of gasoline as well as the power requirement for differing drone weights. As the comparison between the two drones must be carried out under the same conditions, a weight of 20 kg was taken for the drone. This weight constitutes to a gasoline consumption of 1.92 L/h at stationary flight (14 m/s).

Reaction 3.1 provides evidence of the significant emissions produced during operation. However, it is interesting to compare the efficiency of the two drones to assess whether there is a large difference, with a future work focus being the potential improvement of these.

To determine the overall power efficiency of the combustion engine hybrid, the expended power for the drone was utilised along with the minimum power requirement. The minimum power requirement changes depending on the speed and pitch angle, the calculation for which along with required parameters is exhibited in *Appendix 0*.

$$P = \frac{P_{min}}{\eta} \quad \text{Equation 3.8}$$

As the expended power requirement for the drone was included within the data provided by *Quaternium*, the efficiency can be estimated by rearranging the equation.

$$\eta = \frac{P_{min}}{P} \quad \text{Equation 3.9}$$

4.4 Emissions Produced

As mentioned, the consumption of fuel is the primary contributor to emissions. When analysing this contribution of emissions, there were two sources considered: those produced during operation and those produced through fuel (octane oil and hydrogen) production.

4.4.1 Emissions Produced during Operation

The emissions produced during flight for each drone must be evaluated to generate a fair comparison. Despite drones being proposed as a transportation method with reduced greenhouse gas emissions, the different drone energy models produce widely divergent emissions.

For the fuel cell model drone, there are no emissions produced directly during operation. This is due to the reaction taking place within the PEMFC producing only non-harmful products, as shown in *Section 3.8.3*.

In contrast, the combustion engine powered drone does produce carbon dioxide (CO₂), displayed within the *Reaction 3.1*. This can be calculated one of two ways. The first is by taking the fuel consumed and estimating the amount of CO₂ which is approximately released per litre, allowing an averaged amount of CO₂ release can be summed. An estimation of the emissions released was taken from literature, where for 1 L of petrol burnt there is approximately 2.3 kg of CO₂ released (Anon n.d.).

An alternative method for calculating emissions produced during flight for the combustion engine hybrid drone is to use the flowrate of fuel and a molar balance technique with respect to *Reaction 3.1*. The two methods were compared to suggest an accurate emission production during drone operation.

4.4.2 Emissions Produced through Fuel Production

As the gasoline production method is consistent worldwide, the emissions for this fuel were taken to be constant for the amount required during drone operation. However, on the contrary there are a variety of production methods for hydrogen which all have varying emissions contributions. These can range from the steam reforming of natural gas to the electrolysis of water.

4.4.2.1 Environmental Impact Assessment of Hydrogen Fuel Production Sources

The production of hydrogen efficiently, at minimum cost and in an environmentally acceptable manner is crucial for the development of sustainable energy sources. Currently, there are commercial processes that produce hydrogen for a variety of uses such as the chemical sector, hydrocracking, and aerospace industry.

The long-term goal of hydrogen economy is the production of hydrogen from carbon-free or carbon-lean energy sources including renewable electricity and biomass. This climate-neutral hydrogen is termed 'green hydrogen'.

Grey hydrogen is most common, generated from natural gas or methane through a steam reforming process. This process generates a small, but still significant, measure of emissions. These grey hydrogen processes often use gasification technology, with methane or coal as the fuel source.

Blue hydrogen is wherever the carbon generated in the process is captured and stored underground through industrial carbon capture and storage (CSS). This particular hydrogen is referred to as 'low carbon' as it is almost completely impossible to capture all hydrogen produced, with 10-20% escaping to the atmosphere and contributing to emissions (Ji and Wang 2021; Kothari, Buddhi, and Sawhney 2008).

4.5 Autonomy of Both Designs

The range of flight for the drones is the length of time which it is able stay at constant flight without the need for intervention. The drone time in flight can be limited by the amount of fuel on board, but there also has to a balance between the weight of the drone and the energy availability on board. By increasing the fuel quantity on board, the energy availability and weight of the drone increase. This flight time is also termed the flight autonomy, and by increasing this the drone can travel greater distances, thus being more applicable for industry use.

To evaluate the flight autonomy of both drone types, the dynamic response of the system was conducted against semi-empirical demand curves of the drone in terms of the current intensity required. The demand curves display the relationship between the current intensity and power requirement over the duration of the flight. These curves involve assumptions and approximations used to simplify the calculation for the intensity requirements during the drone flight. Assuming a constant voltage, the trends seen in experimental data, as well as that from simulation results, were manipulated to construct a demand curve for each drone. As the current intensity and voltage of each drone was known, the power requirement could be calculated at each point of flight.

When producing the demand curve displaying the contribution of each component, it was known that the battery was required for the peak loading during the take-off and landing phases. There was also evidence which suggested that the ICE-EG was unable to produce a current greater than 30 A, and so the battery was required throughout operation as the drone demand exceeded this (Krznar and Piljek 2021). It should be made clear that these demand curves are an estimation of the requirements throughout flight in order

to compare the flight autonomy of both drones. To make these more accurate, both drones would have to be operated under same conditions and an analysis of the fuel consumption and battery charge would need to be carried out.

The demand curve displays the time, current intensity, and power of the drone. The curve is based on the voltage range reached by the power source and LiPo battery in each case, allowing the energy requirement of the drone to be translated directly and converted into a demand for the electric current intensity.

In essence, the operating requirements of the battery were established based on the flight of each drone at each instance in time, which is illustrated using the demand curves. Any flight path which is carried out can be divided into 5 phases (start, take-off, continuous flight, landing and stop) which are characterised by an approximate period of time and an established consumption range. The description of these flight phases can be found in *Appendix 0*.

5 RESULTS AND DISCUSSION

Within this section, data collected for result analysis was obtained using methodology outlined in *Section 4*. For each of the two points of comparison, data involved is presented with a discussion of what this suggests in terms of both the emissions produced and the flight autonomy.

5.1 Fuel Consumption

The consumption of the octane 95 oil, a type of gasoline, was included in the data which was provided by *Quaternium*. This meant the flowrate of consumption, which both emissions produced and flight autonomy ultimately rely upon, did not require further action.

However, the consumption of hydrogen did. The method for this was defined in *Section 4.2.*, with the volumetric flow of hydrogen required under standard conditions determined to be a value of 1603 L/h. This value was obtained through the simulation performed by the university before commencement of the project.

Table 4- Volumetric flow of hydrogen consumption under storage conditions

Parameter	Definition	Value
Q_{H_2}	Volumetric Flowrate of Hydrogen (Storage Conditions)	7 L/h
Q_{H_2N}	Volumetric Flowrate of Hydrogen (Standard Conditions)	1603 L/h
F_{H_2}	Molar Flowrate	0.706 mol/h
R	Ideal Gas Constant	8.3145 (atm.L/mol.K)
T_{H_2}	Storage Temperature	298 K
P_{H_2}	Storage Pressure	296 atm
T_N	Standard Temperature	273 K
P_N	Standard Pressure	1 atm
Z_{H_2}	Compressibility Factor (Storage Conditions)	1.2
Z_N	Compressibility Factor (Standard Conditions)	1

As can be seen from *Table 4*, the volumetric flowrate of hydrogen for stationary flight has a value of 7 L/h, meaning for the purpose of the one-hour flight time 7L of hydrogen is required.

5.2 Drone Efficiencies

5.2.1 Fuel Cell Efficiency

The input data and parameters provided by simulation allowed for the fuel cell energy conversion efficiency to be calculated, with required parameters as well as the results displayed in *Table 5*.

Table 5- Fuel cell energy conversion efficiency

Parameter	Definition	Value
Input Data		
I_{out}	Converter Output Current (A)	10
V_{out}	Converter Output Voltage (V)	20
Input Parameters		
P_0	Constant (V)	0.5
U_s	Voltage Set-point (V)	0.1
R_l	Internal Electrical Resistance (ohm)	0.05
Output Data		
P_{out}	Output Power (W)	200
P_{loss}	Power Losses (W)	6.5
P_{in}	Input Power (W)	206.5
I-V Curve of Fuel Cell		
T_{stack}	Stack Temperature (K)	343
P_{H_2}	Hydrogen Pressure (bar)	0.8
P_{O_2}	Oxygen Pressure (bar)	1
N	Number of Cells	20
$[O_2]$	Adjusted Oxygen Concentration (mol/cm ²)	8.41E-07
T_{mem}	Membrane Thickness (cm)	0.0118
γ	Wetting Condition of Polymeric Membrane	0
A_{mem}	Membrane Area (cm ²)	232
Results		
E	Thermodynamic Cell Potential (V)	1.188
η_{ohmic}	Voltage Losses in Ohmic Region (V)	-0.29
η_{act}	Voltage Losses due to Activation (V)	-0.01
U_{cell}	Output Voltage (V)	0.89
U_{TH}	Thermoneutral Voltage (V)	1.48
η_e	Conversion Efficiency of the Fuel Cell (%)	60

As is shown, the fuel cell has a theoretical efficiency of 60%, obtained using *Equation 3.1*, which corresponds with the typical efficiency range of a PEMFC.

5.2.2 Combustion Engine Efficiency

As the power requirement for the drone for different weights was provided by *Quaternium (Appendix 0)*, the efficiency can be determined using methodology outlined. Data was taken for a drone averaged at

20kg in weight at a stationary speed of 14 m/s. *Figure 8* displays the drone specifications used to determine the minimum power requirement of the drone.

Parameters used to calculate drone efficiency are displayed in *Table 6*. The drag coefficient of 0.8 was estimated using literature sources which estimated the drag coefficient of a large drone (Krishnaraj n.d.; Polivanov and Sidorenko 2021; Stolaroff et al. 2018).

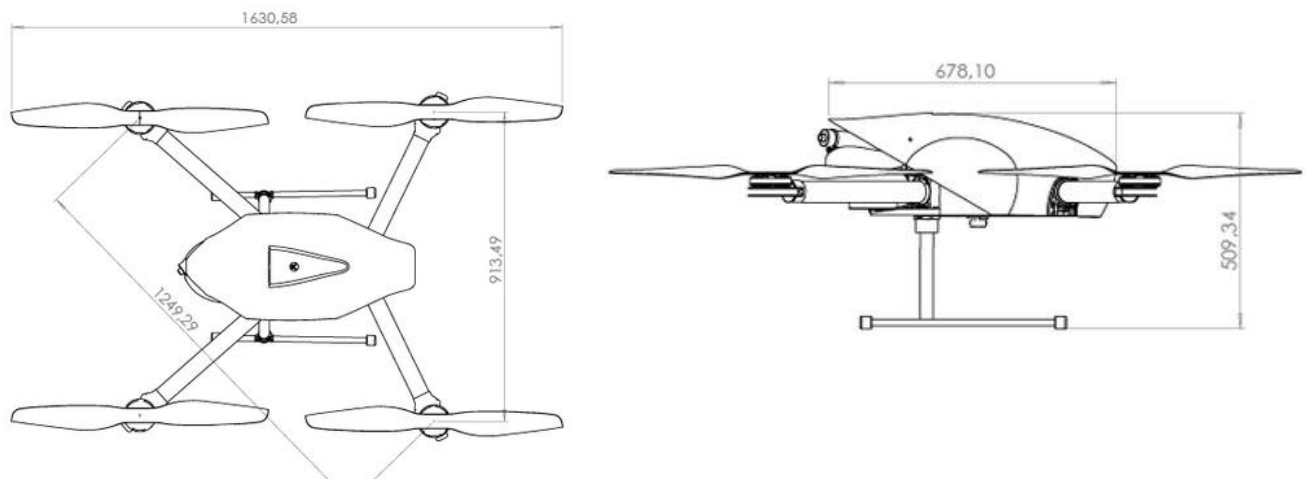


Figure 8- Drone measurement specifications (Quaternium 2021)

Table 6- Combustion engine-battery hybrid efficiency

Symbol	Parameter	Value
C_D	Drag Coefficient	0.8
F_{drag}	Drag Force (N)	79.9
α	Pitch Angle (Radians)	0.39
TH	Thrust (N)	276.09
$P_{min, hover}$	Minimum Power Requirement, Hovering (W)	5834944.04
P_{min}	Minimum Power Requirement (W)	1213
η	Efficiency (%)	56

As shown, the overall efficiency of the combustion engine drone is 56%.

5.3 Emissions Production

5.3.1 Emissions Produced during Operation

As explained, two methods were adopted to determine the quantity of CO₂ produced during operation of the combustion engine hybrid drone. Method 1 was conducted using data from literature where for every litre of gasoline burned, approximately 2.3 kg of CO₂ is produced (Anon n.d.). Method 2, adopted for further comparison, utilised the complete combustion reaction. This indicates that for every 2 moles of octane 95 consumed, 16 moles of CO₂ are released. Utilising the flowrate of fuel consumption, and

taking the density of fuel as 750 kg/m^3 (Anon n.d.), CO_2 emissions can be determined. *Table 7* displays the results of these calculations and shows a consistency between results from both methods.

Table 7- Emissions produced during operation of combustion engine-battery hybrid drone

Approx Fuel Consumption (L/h)	Mass Flowrate (kg/h)	CO ₂ Produced (kg/h)	
		Method 1	Method 2
2.3	1.725	5.33	5.29
1.2	0.9	2.78	2.07
0.7	0.525	1.62	1.21

As no emissions are produced by the fuel cell hybrid drone, it is concluded that during operation, there are significantly more emissions produced by the combustion engine drone.

5.3.2 Emissions Produced through Fuel Production

To make the evaluation of emissions produced by each drone impartial, those generated through fuel production must be considered. To produce gasoline, there is one major process adopted, referred to as ‘cracking’, for production meaning that the emissions from fuel production are given a constant value.

On the other hand, there are a variety of production methods for hydrogen with varying emissions contributions. With many process options, the most common as well as those with the biggest disparity in emission production were selected to illustrate these variances. Data was acquired from online sources which estimated quantities of CO_2 produced for the processes. An average was taken from this data, and thus results presented are not exactly accurate but are an estimation which allow the differences in emission generation by different production methods to be presented. *Figure 9* displays the quantity of emissions produced through different production methods of hydrogen. These processes were selected due of their clear varying environmental impact, alongside being the most used at present.

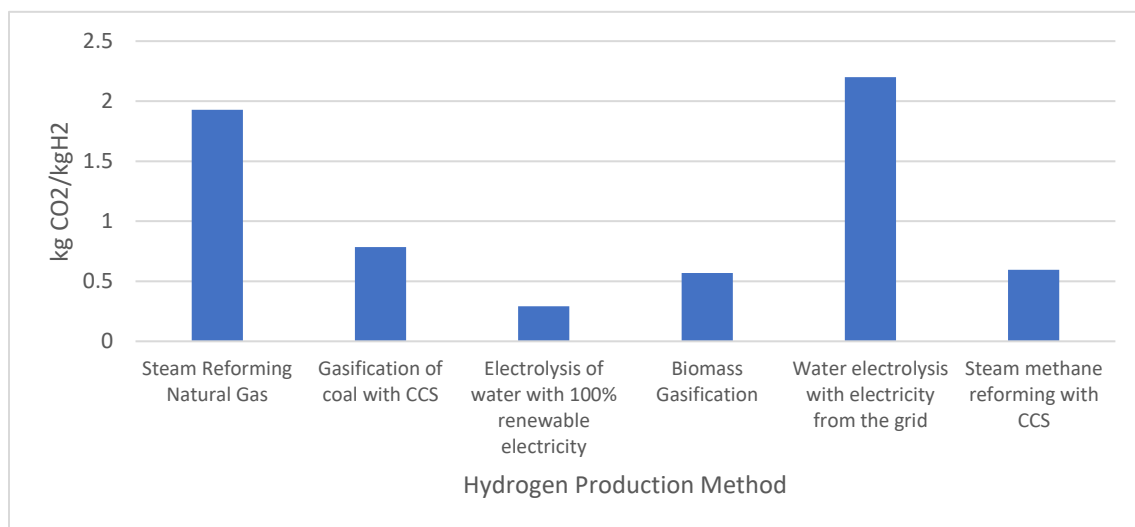


Figure 9- Emissions produced through hydrogen production methods (21,22)

production method of water electrolysis but with differing electricity sources has a notable influence on the CO_2 produced. The use of grid electricity appears to have the biggest environmental impact, whilst

that which utilises renewable energy sources has the lowest. For this instance, it should be noted that the emissions produced from grid sourced electricity is highly dependent on the country from which it is sourced. The impact which the origin country has on this is displayed in *Figure 10*. For this environmental impact assessment of hydrogen production methods, emissions produced throughout the EU in 2020 was used, resulting in a CO₂ production of 2.2kg for fuel required in an hour-long flight.

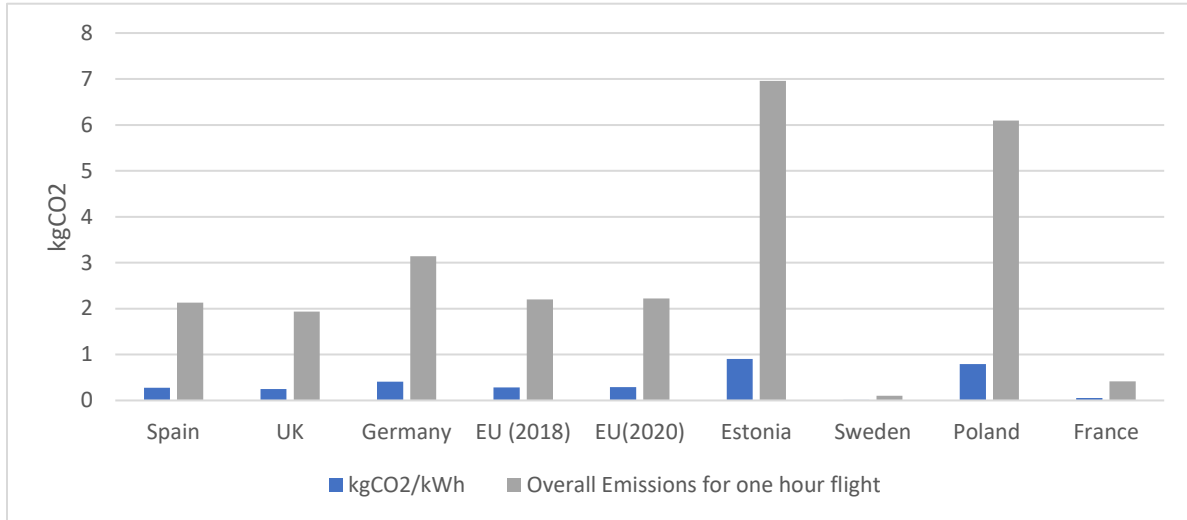


Figure 10- Emissions produced by country's grid electricity (26)

5.3.3 Comparison of Overall Emissions

To complete an estimation of the net emission savings which could be achieved from replacement of the combustion engine with a hydrogen fuel cell an overall comparison of the emissions needs to be made. This can be seen in *Figure 11*, with different hydrogen production methods included to clearly display the impact which can have.

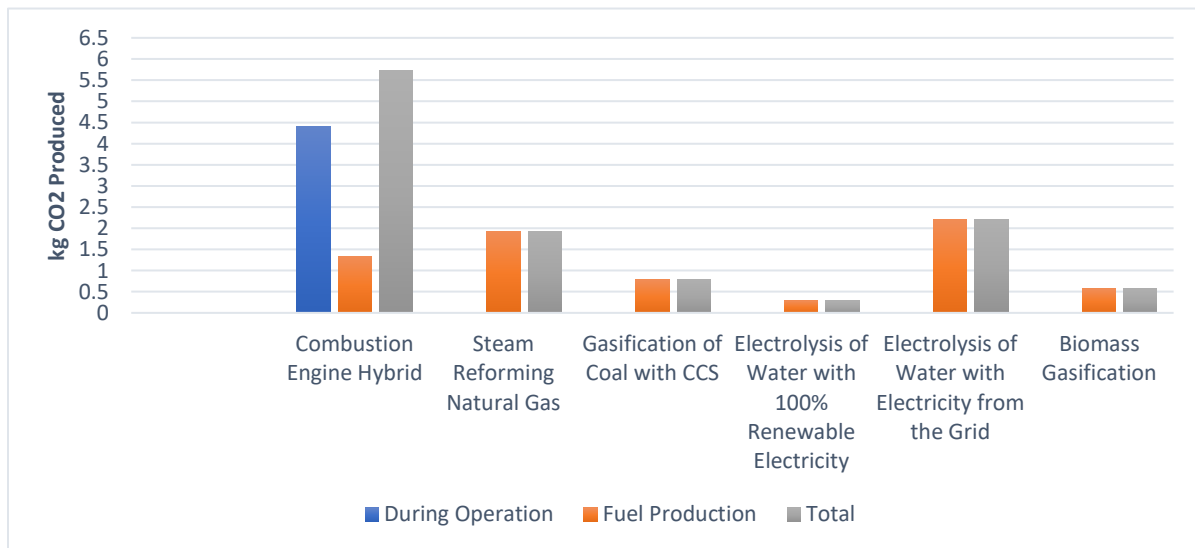


Figure 11- Comparison of emissions produced by each production method

The figure above highlights that the combustion engine hybrid has a larger production of emissions than the hydrogen fuel cell hybrid. However, the graph also emphasizes some interesting points. It is widely assumed that using hydrogen fuel is a more sustainable and environmentally friendly alternative to fuels such as gasoline or diesel. While this is most definitely the case, the production method for the hydrogen fuel has a great impact.

The electrolysis of water using renewable electricity is a green hydrogen production method, yet still contributes a small quantity of emissions due to the water purification. However, as can be seen these are minute in relation to other production methods. Despite this method clearly being the least environmentally detrimental, it is infeasible to produce large industrial quantities of hydrogen. This is due to the large costs required for this type of electricity, which are unattractive when there are much cheaper options available.

With this infeasibility, it would be wise to choose a more commonly adopted production method for hydrogen production for the net emission savings estimation. Steam reforming natural gas is the most widely used, accounting for around half of the world's hydrogen production (Franchi et al. 2020).

Using the emissions from the steam reforming natural gas process to estimate the net emission savings which could be achieved by replacing the combustion engine by a PEMFC suggests a total reduction of 3.8 kg of CO₂ per hour of flight.

5.4 Comparison of Flight Autonomy

As explained, the flight autonomy of a drone is the length of time which it is able to stay in flight without the need for human intervention such as battery recharging or refuelling. To effectively compare the flight autonomy of both drones, a semi-empirical demand curve was constructed. These demand curves allow for the drone requirements at different phases of flight to be displayed. These requirements as presented in two different forms to see both the trend of power requirement with current intensity, and the role of both the battery and primary power source during each phase. The drone flight is split into 5 phases, which are outlined in *Appendix 0*.

For the demand curve of the fuel cell hybrid, the data acquired through simulation and a small drone test flight was manipulated for a drone weight of 20 kg and a flight time of 1 hour. That for the combustion engine hybrid was estimated using a real-life flight trend, where the trends were adapted for the specifications of the *Hybrix 2.1* drone by *Quaternium*.

During the visit to *Quaternium*, the discussion of these demand curves raised some interesting points. Whilst the hydrogen fuel does not weigh a considerable amount, meaning its consumption has practically no effect on the overall weight of the drone, this is not the case for the combustion engine hybrid. The gasoline fuel contributes to a substantial fraction of the drone weight, almost 1.5 kg for an hour-long flight. Therefore, as the fuel is consumed the drone decreases in weight. To account for this weight decrease, a power-weight ratio of 96 W/kg was applied (Rajendran et al. 2016). The weight decrease was applied using the flowrate of gasoline consumption was taken from the overall drone weight, with this being calculated for the consumption every 5 seconds. The decrease in power consumption therefore led to a decrease in the intensity requirement of the drone, as it was assumed that the drone operated at a constant voltage.

The demand curves display similarities in shape, however there are distinct disparities spotted.

5.4.1 Fuel Cell Hybrid Demand Curve

It can be seen for the following demand curve the boot phase has a small requirement before lift-off phase commences. The starting systems require a current intensity of 2A during the initial and final moments of operation, equating to around 80W of power. The maximum demand peaks of the drone are reached

during the take-off and landing phases, approximately 3000W of power and 80A of current intensity. The average stationary flight demand of the drone is seen to be around 2100W of power and 50A of current intensity.

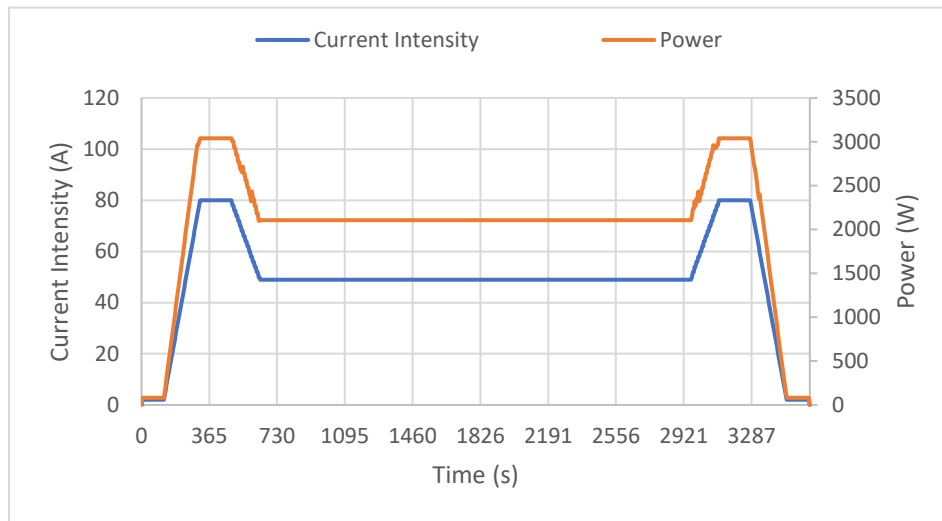


Figure 12- Demand curve for fuel cell-battery hybrid

In terms of current intensity, the optimal point of operation in constant regime for the PEMFC was established using simulation results, and the LiPo battery used as an auxiliary support system to reach the consumption peaks during the take-off and landing phases of the drone. These peaks are seen because of the need for the drone to ascend and descend in a controlled manner, causing an increase in requirements. This can be seen in Figure 13..

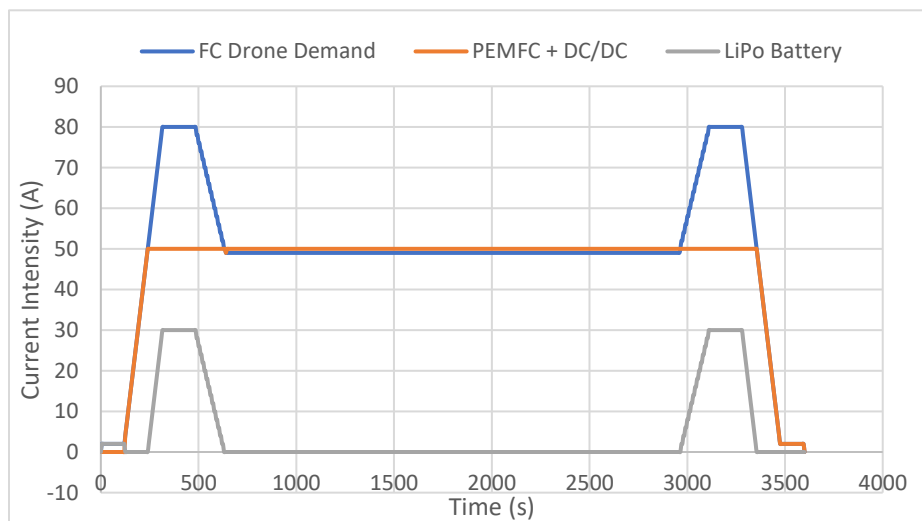


Figure 13- Modelling of hybrid system 'PEMFC + LiPo'

At the beginning of the drone operation ($t < 1\text{min}$), the LiPo battery is solely responsible for providing the 2A essential for initialisation of the drone's starting systems and to supply the balance of the plant required by the fuel cell. Afterwards, the power supply of the balance of the drone is self-sufficient with the current generated by the fuel cell.

The PEMFC+DC/DC reaches a constant operating regime of approx. 51A, with the LiPo battery providing the remaining 30A to achieve the maximum peaks of 80A during the take-off and landing phases. It is observed during the stationary flight phase, the PEMFC+DC/DC generates a slight energy surplus in the form of electric current (+1A) used for recharging the LiPo battery.

5.4.2 Combustion Engine Hybrid Fuel Cell

Similarly for the combustion drone demand curve the LiPo battery provides the initial current, or in this case the 'DC bus load' until the electrical generator can take over. For the situation analysed it was assumed that the regimes were medium-high load, equivalent to 1-2 Ω . The voltage reference for this drone was set to 50V (Krznar and Piljek 2021). The average generator current is around 30A, corresponding to 1500-1750W of power consumption.

The DC bus voltage is maintained at the target value of 50V, however due to the change in weight with fuel consumption the power requirement decreases during operation. To account for this change, the fuel consumption per second was calculated to be 0.0024 kg, and taken away from a start weight of 21 kg. A weight-power ratio of 96 W/kg was applied to calculate the power requirement, where the fuel consumption which contributes to the weight decrease was factored in (Rajendran et al. 2016). It was assumed, from literature data, that consumption of fuel is linear and is not impacted by different requirement in flight phases (Krznar and Piljek 2021). Although this realistically is not the case, without the ability to carry out a sample flight to calculate the rate of consumption this was the best available technique.

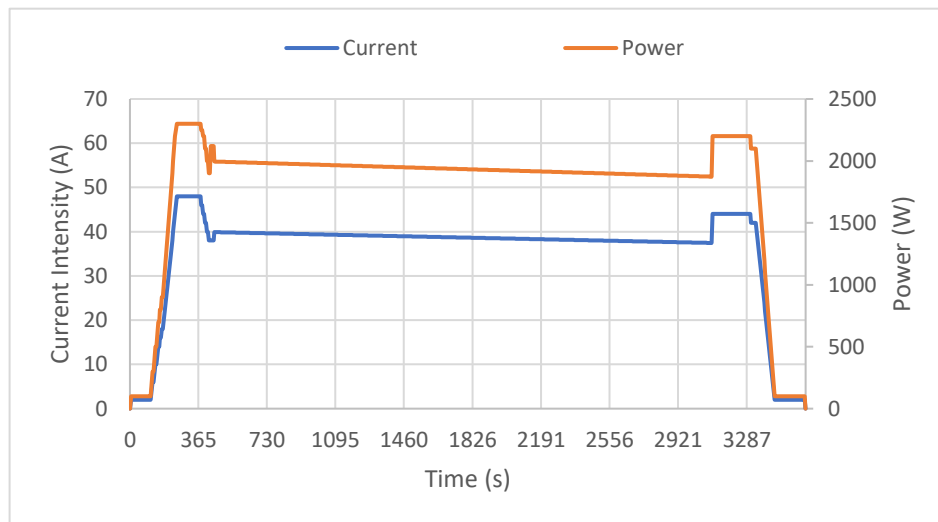


Figure 14- Demand curve for internal combustion engine-battery hybrid

The maximum demand peak is seen towards the lift off and landing phases of flight, with the overall hybrid power system being characterised by the maximum power production of 2300W. This power output was selected as it is the maximum required for a 'large drone' of 20kg in weight, according to data analysed from *Quaternium*. With larger power requirements for larger loads, the LiPo battery supplies the additional peak load. This is required because of the limited internal combustion engine-electrical generator power output of approx. 30A, resulting in the battery supplying additional current. As the 30A peak limit for the generator is reached, the battery which exhibits variations in current. These variations are due to the direct relationship between the current and power, assuming that a constant voltage of 50V is applied for the duration of flight.

There are slight discrepancies which can be seen in the drones, where the slope is not a perfectly straight line. This is due to the operation being carried out for a real flight, unlike a theoretical one such as that simulated for the fuel cell. These variations are caused by real flight conditions, as the reaction of the drone would not be perfectly carried out with different factors such as wind, maintaining stationary flight etc. having to be taken into consideration.

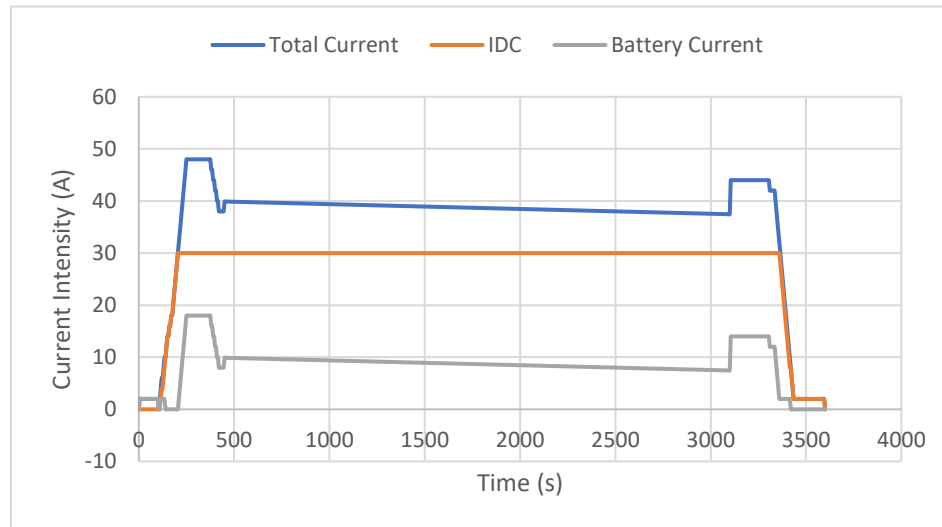


Figure 15- Modelling of the hybrid system 'ICE + LiPo'

The demand curves show that for an average flight weight of 20kg, with the same flight conditions, the combustion engine drone has a lower demand and therefore a better flight autonomy. The demand curves display the current intensity as well as the power requirement throughout flight, and it is seen that these are lower throughout flight for the combustion drone. This aligns with the current technology available, as seen in the commercial drones, as the combustion drone can stay in flight longer than the fuel cell drone.

5.5 Battery Specifications

The battery must allow for the transport of additional load without compromising the energy demand of the drone.

Sizing of the LiPo battery must consider the voltage range provided by the primary power source of the drone. It must meet the minimum requirements of the hybrid system, ensuring that the criteria is complied with whilst ensuring minimum size and weight to increase energy density. The LiPo battery must allow the drone to reach the maximum peaks of electrical consumption during take-off and landing phases for the PEMFC hybrid drone, and the additional requirement for the combustion engine hybrid. It can be concluded that the LiPo battery must have sufficient energy capacity and discharge rate to provide the necessary electrical power for each drone, but also maintain a minimum discharge fraction of 20-30% after the full flight of the drone. The requirements for each battery can be seen below, with the number of cells and minimum rated voltage included.

To determine the minimum energy capacity of the battery, the worst-case scenario was considered. This is the point where the battery has the highest possible demand to ensure in the event of any flight issues, there is sufficient energy left within the battery to carry out a safe landing. For this, the demand curves were analysed for the current requirement sourced from the battery. The current intensity demand for each drone was summed across the hour-long operation, allowing the overall energy capacity to be

estimated. The minimum energy capacity which meets the criterion of the minimum load fraction was estimated, as shown in *Table 8*.

The voltage of the battery was determined based on the number of cells, identified by the ‘S’ count. Data for the specifications of the battery was obtained from existing commercial Lithium Polymer batteries which meet the characteristics for the requirements of each drone. Therefore, by knowing the battery used by *Quaternium* is 6S, with 6 cells, the rated voltage must be 22 V. This battery is based on the commercial *Kylinpower* LiPo battery *KP10000-6S model* (Anon n.d.) . The fuel cell battery is based on the commercial model *HRB GRAPHENE 10S-3000 model* due to its low weight and reliability (Anon n.d.). As can be seen the weight of the combustion engine hybrid battery is greater than that of the fuel cell hybrid. This is due to the greater additional power demand provided by the battery as the 30 A limit is reached and surpassed during flight.

Table 8- Battery Specifications

	Fuel Cell Battery	Combustion Engine Battery
Number of Cells	10S (5S + 5S)	6S
Energy Capacity	3000 mAh	10000 mAh
Rated Voltage	37V	22 V
Maximum Load Ratio	2C	25C
Maximum Discharge Rate	100C	50C
Net Mass	876 g	1400 g

5.6 Areas of Difficulty

Whilst performing a study of the background and current technology for drones, it became apparent that certain stumbling blocks would be met. From the early stages of the project, my lack of experience with the simulation environment TRNSYS (Transient System Simulation Program) was highlighted as a potential issue which could prevent desired progress. This software allows modelling and simulation of complex dynamic systems through the interconnection of modular structures implemented internally in the program library. However, the program takes time to understand and master, time which was not available within the project timeline. To overcome this, existing simulation data which had been acquired by the university was adapted for the specifications required using Excel.

As the project progressed, the modelling of a combustion engine hybrid drone became an area of concern as information was lacking in much research and there was no inbuilt simulation environment which would allow for the theoretical modelling. There was a severe lack of information available on the inner workings of the combustion engine drone, most likely due to commercial confidentiality. Fortunately, the department have contacts within a nearby company, *Quaternium*, who work on combustion engine hybrid drones. This connection led to a visit to the company, allowing me to see first-hand how such drones are manufactured, and an agreement was reached to pass on drone data for the drones essential for the project progression.

5.7 Future Work Opportunities

From the data analysis and the results obtained, it is evident there is a great scope for further research.

Advancements of the results obtained could determine the influence varying tank size designs have on the flight autonomy and emissions production. For this project, the fuel tank sizes were assumed to provide the fuel required for a one-hour flight time. However, it would be interesting to see how varying fuel quantity would affect other on-board parameters. Understanding how the drone behaves with

different tank sizes and under different operating conditions could enable a sensitivity curve to be constructed to help aid with future projects.

An investigation could be carried out into how an increase in range compare between the two technologies. As was mentioned previously the balance between the two opposing requirements must be achieved: the need for sustained power production (energy capacity) to achieve flight endurance, and the need for peak load levelling to achieve satisfactory in-flight dynamic performance. In this sense the demand curves produced for this project could be used as a starting point for different demand curves which display different sizes, designs and different intensity distributions between the battery and power source. This would allow for a greater understanding of the drone potential have, and how developments could be made to make the most efficient and sustainable transportation method possible.

It would also be interesting to study different variables which could improve the efficiency of each drone power system. As the maximum theoretically achievable efficiency is 60% for the fuel cell, it would be interesting to test how different fuel cells work under the conditions and whether this would make a significant improvement on the flight autonomy. It could also be useful to assess different variables which improve the combustion engine efficiency, such as increasing the oxygen intake for the combustion reaction.

Currently, the recharging of the LiPo battery is blocked by the diode in the combustion engine system configuration displayed in *Figure 2*. This is used to prevent uncontrolled battery charging from the power distribution system, and related battery current and voltage overloads. It would be interesting to explore the hybrid power supplies which feature energy recovery much like the fuel cell hybrid. This would allow battery recharging if the generated power of the hybrid drive were to allow it, by means of the power distribution system and battery current control. This could require additional power electronics systems in the form of a bidirectional power convertor. Successful research and implementation of this could result in a lighter battery, and thus a reduced overall drone weight with associated potential decrease in emission production and better flight autonomy.

6 CONCLUSIONS/OUTCOME

The study and analysis of data obtained for two hybrid UAVs allowed for a comparison to be completed in two key areas of interest. The hybrid systems included a polymeric exchange membrane fuel cell (PEMFC) and an internal combustion engine – electricity generator (ICE-EG), both fitted with a LiPo battery. Essential data was collected for the study of the PEMFC hybrid using the simulation program TRNSYS alongside a small drone test flight, conducted by the university prior to the commencement of this study. The data collected for the study of the combustion engine hybrid was provided by the drone manufacturing company *Quaternium*, alongside other literature sources which aided the understanding of hybrid systems. Data collected was manipulated for a flight time of 1 hour with a 20kg drone carrying out a stationary flight, which allowed for the flights of both hybrid systems to be compared. Being unable to obtain data from a real-life flight of 20 kg for both drones meant that it had to be assumed that the discrepancies between the simulated data and that taken from commercial models would still allow for a fair comparison. For a more accurate comparison, however, it would have been necessary to assess the flight of two drones which was unfortunately not possible during the project timeline.

The two hybrid systems studied are commercially available, and were analysed to compare emissions as well as their flight autonomy. The combustion engine hybrid had a fuel consumption flowrate of 1.92 L/h and the hydrogen fuel cell hybrid had a higher fuel consumption rate of 7 L/h. These volumetric flowrates were then used to estimate the emissions which would be produced by each drone during an hour-long stationary flight. The drones follow different trends regarding the weight throughout operation. The compressed hydrogen weighs very little- and as a result it was assumed that the decrease of this would be insignificant to the overall drone weight. However, the gasoline weight equates to 1.44 kg- meaning as it is consumed the drone weight will decrease. This weight difference was factored into the drone requirements by applying a power-weight ratio of 96 W/Kg for gasoline consumption over an hour-long flight.

The approximation of the flight autonomy needed the power requirement and current intensity to be determined for the different phases of flight, outlined in *Appendix 0*. The result demonstrates that although both drones follow a similar trend, where the LiPo battery is required for start-up and landing phases, there are inconsistencies. The combustion engine drone has a slight decline during the stationary phase, as a result of the consumption of the heavier gasoline fuel. The role of the battery in each hybrid system also differs. During flight the battery is only required during the take-off and landing phases for the fuel cell hybrid, whereas the battery use is sustained throughout for the combustion engine drone.

In terms of the requirements for each drone, the fuel cell sustains a higher power and current intensity for the entire flight. The combustion engine hybrid therefore has a greater energy density; however, it does require a larger battery due to the greater additional power requirement. With the greater energy density, it is understood that the combustion engine hybrid has a better flight autonomy and so is capable of maintaining flight for a longer period without the need of human interference. This coincides with the commercial models as the *Quaternium* internal combustion hybrid drone has a maximum flight time of 4+ hours, whilst the *HES Energy Systems* hydrogen fuel hybrid drone has a lower potential maximum flight time of 3.5+ hours.

It is estimated that there would be a net emissions saving of 3.8kg CO₂/h should the combustion engine hybrid be replaced by a hydrogen fuel cell. This value is dependent heavily on the production method for the hydrogen fuel, with the potential to make greater emission savings with a more environmentally friendly process adoption.

7 REFLECTION AND REVIEW

Undertaking this Erasmus placement in Valencia has given me the opportunity to both live and study in an unfamiliar country. The experience has been invaluable, allowing me to develop both professionally and personally. The research I have carried out at UPV allowed me to apply much of the chemical engineering knowledge and experience I have gained from my years at Strathclyde University. The work is also extremely beneficial in aiding the current goal of moving towards a carbon neutral society. The production of emissions contributing to global warming and other environmental issues is at the forefront of research worldwide, and with transport emissions being such a major contributor it is essential that more sustainable methods be developed. It was a privilege to be able to be involved in this type of research and to contribute to further research within the area.

From commencement of the project my personal goals and aims were to:

1. Further my knowledge on UAVs and the challenges faced within the industry
2. Gain experience working with an academic research team and apply theoretical knowledge to real scenarios.
3. Demonstrate the ability to work independently, problem solve, manage, and maintain a project plan, and overcome any communication and language barriers faced.

Reflecting on my experiences here at the UPV I feel my personal goals were achieved through efficient time management, planning and active communication with my supervisor. My unfamiliarity with the topic meant time had to be taken in the initial stages to fully understand drones and their inner workings, meaning I had to plan my time wisely. I made sure that as soon as I had a fundamental understanding I progressed with the project, completing background research as well as initiating data collection for analysing. This showed my initiative, motivation, and willingness to learn from the project outset.

I was able to gain a deeper understanding of drones and the possibilities they present. My understanding was developed by carrying out a literature review, both through my own research and that carried out within the department. Having access to so much knowledge on the subject from a variety of different sources allowed me to communicate with various department members to gain additional insight into the subject. During this time, it became clear that a trip to *Quaternium* would be required for the progression of the project, and the department organising this for myself was massively appreciated. Overall, the project has taught me the importance of communication and collaboration with various people both in UPV and at *Quaternium*, especially with such specialist knowledge available.

During my time here I have been able to build upon theory and skills I learned during my undergraduate studies. First and foremost, Electrochemical Energy Devices aided me with a fundamental understanding of the background theory behind the hydrogen fuel cells. It was interesting to put this theory into practice within the project background when determining the theoretical efficiency of the hydrogen fuel cell. The Clean Combustion Technologies course also allowed me to have a basic understanding of the reactions taking place within the combustion engine hybrid drone, which played a key role in the calculation of emission production. I was able to handle the project scheduling effectively by creating a plan and determining in advance the critical deadlines using knowledge gained from the Chemical Engineering Design Project undertaken in the previous year. I made sure that an academic logbook was kept with any daily analysis results detailed alongside what I was learning.

The biggest personal challenge I faced was adapting to a new culture and lifestyle. I was lucky enough to have a supervisor who, despite being a native Spaniard, spoke fluent English, which helped considerably. Despite this, completing this project in Spain brought me into an unfamiliar working culture. This acclimatisation was challenging to begin with however as I developed my own understanding of Spanish and became used to working routines, I found myself enjoying both my project work and living in Valencia.

8 BIBLIOGRAPHY

- Anon. 2016. '20.2: Standard Entropy'. *Chemistry LibreTexts*. Retrieved 15 February 2022 ([https://chem.libretexts.org/Bookshelves/Introductory_Chemistry/Introductory_Chemistry_\(CK-12\)/20%3A_Entropy_and_Free_Energy/20.02%3A_Standard_Entropy](https://chem.libretexts.org/Bookshelves/Introductory_Chemistry/Introductory_Chemistry_(CK-12)/20%3A_Entropy_and_Free_Energy/20.02%3A_Standard_Entropy)).
- Anon. n.d. 'Automated Drone (UAV) Applications'. *Airobotics*. Retrieved 4 February 2022 (<https://www.airoboticsdrones.com/applications/>).
- Anon. n.d. 'Grotthuss Mechanism - an Overview | ScienceDirect Topics'. Retrieved 28 January 2022 (<https://www.sciencedirect.com/topics/engineering/grotthuss-mechanism>).
- Anon. n.d. 'How Electricity Is Generated - U.S. Energy Information Administration (EIA)'. Retrieved 11 April 2022 (<https://www.eia.gov/energyexplained/electricity/how-electricity-is-generated.php>).
- Anon. n.d. 'HRB GRAPHENE 10S 3000 37V 100C LIPO BATTERY EC5'. Retrieved 31 March 2022 (<https://hobbyshop247.com/10S-3000-37V-100C-EC5>).
- Anon. n.d. 'HYBRiX20 RTF – Quaternium'. Retrieved 3 March 2022 (<https://www.quaternium.com/hybrix20-rtf/>).
- Anon. n.d. 'Internal Combustion Engine Basics'. *Energy.Gov*. Retrieved 13 April 2022 (<https://www.energy.gov/eere/vehicles/articles/internal-combustion-engine-basics>).
- Anon. n.d. 'Kg CO2 per Litre of Petrol Vehicles'. *Comcar*. Retrieved 14 March 2022 (<https://comcar.co.uk/emissions/co2litre/>).
- Anon. n.d. 'Kylinpower 10000mAh 6S 22.2V 25C Lipo Battery for UAV Multicopter Drone - KylinPower'. *Https://Www.Wskylin.Com/*. Retrieved 31 March 2022 (<https://www.wskylin.com/product/kylinpower-10000mah-6s-22-2v-25c-lipo-battery-for-uav-multicopter-drone/>).
- Anon. n.d. 'Stroke Cycle - an Overview | ScienceDirect Topics'. Retrieved 11 April 2022 (<https://www.sciencedirect.com/topics/engineering/stroke-cycle>).
- Anon. n.d. 'Technical Specification : 95 Octane Petrol (A0018L99) – CEYPETCO'. Retrieved 14 March 2022 (<https://ceypetco.gov.lk/95octane/>).
- Anon. n.d. 'The Benefits of a 2 Stroke Engine in a Mower - News | PSD Groundscare'. Retrieved 11 April 2022 (<https://www.psdgroundscare.co.uk/news/post/benefits-of-a-2-stroke-engine.html>).
- autam, Rajeev. n.d. '(PDF) Bipolar Plate Materials for Proton Exchange Membrane Fuel Cell Application'. *ResearchGate*. doi: 10.2174/1874464808666150306223104.
- Brightman, E. 2021. 'Electrochemical Energy Devices', University of Strathclyde.
- Chase, M. W. 1998. 'NIST-JANAF Thermochemical Tables, Fourth Edition'. 1–1951.

- Franchi, Giovanni, Mauro Capocelli, Marcello De Falco, Vincenzo Piemonte, and Diego Barba. 2020. 'Hydrogen Production via Steam Reforming: A Critical Analysis of MR and RMM Technologies'. *Membranes* 10(1):10. doi: 10.3390/membranes10010010.
- Grepow. 2020. 'Lipo Battery for Drone: Introduction, Choice And Safety'. *Grepow Blog*. Retrieved 1 February 2022 (<https://www.grepow.com/blog/lipo-battery-for-drone/>).
- Hwang, Myeong-hwan, Hyun-Rok Cha, and Sung Yong Jung. 2018. 'Practical Endurance Estimation for Minimizing Energy Consumption of Multicopter Unmanned Aerial Vehicles'. *Energies* 11(9):2221. doi: 10.3390/en11092221.
- Isanaka, Sriram Praneeth, Austin Das, and Frank Liou. 2012. *DESIGN OF METALLIC BIPOLAR PLATES FOR PEM FUEL CELLS*. Missouri University of Science and Technology.
- Je Seung Lee, and Nguyen Dinh Quan. 2005. *Polymer Electrolyte Membranes for Fuel Cells*. Korea Institute of Science and Technology.
- Ji, Mengdi, and Jianlong Wang. 2021. 'Review and Comparison of Various Hydrogen Production Methods Based on Costs and Life Cycle Impact Assessment Indicators'. *International Journal of Hydrogen Energy* 46(78):38612–35. doi: 10.1016/j.ijhydene.2021.09.142.
- Khotseng, Lindiwe. 2019. *Fuel Cell Thermodynamics*. IntechOpen.
- Kothari, Richa, D. Buddhi, and R. L. Sawhney. 2008. 'Comparison of Environmental and Economic Aspects of Various Hydrogen Production Methods'. *Renewable and Sustainable Energy Reviews* 12(2):553–63. doi: 10.1016/j.rser.2006.07.012.
- Krishnaraj. n.d. 'Aerodynamic Analysis of Hybrid Drone'. *IOP Conference Series: Materials Science and Engineering* 1012(012023).
- Krznar, Matija, and Petar Piljek. 2021. *Modeling, Control System Design and Preliminary Experimental Verification of a Hybrid Power Unit Suitable for Multicopter UAVs*. Department of Robotics and Production System Automation, Faculty of Mechanical Engineering and Naval Architecture, University of Zagreb,.
- Li, Jun. 2021. 'Clean Combustion Technologies', University of Strathclyde.
- Li, Zesheng, Bolin Li, Yifan Hu, Shaoyu Wang, and Changlin Yu. 2022. 'Highly-Dispersed and High-Metal-Density Electrocatalysts on Carbon Supports for the Oxygen Reduction Reaction: From Nanoparticles to Atomic-Level Architectures'. *Materials Advances* 3(2):779–809. doi: 10.1039/D1MA00858G.
- Litster, and Mclean. 2004. 'PEM Fuel Cell Electrodes'. *Journal of Power Sources*.
- Ma, Ruguang, Gaoxin Lin, Yao Zhou, Qian Liu, Tao Zhang, Guangcun Shan, Minghui Yang, and Jiacheng Wang. 2019. 'A Review of Oxygen Reduction Mechanisms for Metal-Free Carbon-Based Electrocatalysts'. *Npj Computational Materials* 5(1):1–15. doi: 10.1038/s41524-019-0210-3.
- Makridis. 2016. 'Hydrogen Storage and Compression'.

- Matthey, Johnson. n.d. 'The Role of Platinum in Proton Exchange Membrane Fuel Cells'. *Johnson Matthey Technology Review*. Retrieved 23 February 2022 (<https://www.technology.matthey.com/article/57/4/259-271/>).
- O'Hayre, Ryan, Suk-Won Cha, Whitney Colella, and Fritz B. Prinz. 2016. *Fuel Cell Fundamentals: O'Hayre Chapter 2: Fuel Cell Thermodynamics*. Hoboken, NJ, USA: John Wiley & Sons, Inc.
- Polivanov, P. A., and A. A. Sidorenko. 2021. 'Aerodynamic Characteristics of a Quadcopter with Propellers'. P. 040053 in. Novosibirsk, Russia.
- Rajendran, Smith, Yahaya, and Mazlan. 2016. 'Electric Propulsion System Sizing for Small Solar-Powered Electric Unmanned Aerial Vehicle'. *International Journal of Applied Engineering Research* 11:9419–23.
- Rosli, R. E., A. B. Sulong, W. R. W. Daud, M. A. Zulkifley, T. Husaini, M. I. Rosli, E. H. Majlan, and M. A. Haque. 2017. 'A Review of High-Temperature Proton Exchange Membrane Fuel Cell (HT-PEMFC) System'. *International Journal of Hydrogen Energy* 42(14):9293–9314. doi: 10.1016/j.ijhydene.2016.06.211.
- Salam, M. Abdus, Md Shehan Habib, Paroma Arefin, Kawsar Ahmed, Md Sahab Uddin, and Tareq Hossain. 2020. 'Effect of Temperature on the Performance Factors and Durability of Proton Exchange Membrane of Hydrogen Fuel Cell: A Narrative Review'. *Material Science Research India* 17(2):179–91.
- Stolaroff, Joshua K., Constantine Samaras, Emma R. O'Neill, Alia Lubers, Alexandra S. Mitchell, and Daniel Ceperley. 2018. 'Energy Use and Life Cycle Greenhouse Gas Emissions of Drones for Commercial Package Delivery'. *Nature Communications* 9(1):409. doi: 10.1038/s41467-017-02411-5.
- Townsend, Ashleigh, Immanuel N. Jiya, Christiaan Martinson, Dmitri Bessarabov, and Rupert Gouws. 2020. 'A Comprehensive Review of Energy Sources for Unmanned Aerial Vehicles, Their Shortfalls and Opportunities for Improvements'. *Heliyon* 6(11):e05285. doi: 10.1016/j.heliyon.2020.e05285.
- UNGAN, Hande, and Ayşe BAYRAKÇEKEN YURTCAN. 2020. 'Water Management Improvement in PEM Fuel Cells via Addition of PDMS or APTES Polymers to the Catalyst Layer'. *Turkish Journal of Chemistry* 44(5):1227–43. doi: 10.3906/kim-2002-49.
- US EPA, OAR. 2016. 'Global Greenhouse Gas Emissions Data'. Retrieved 3 April 2022 (<https://www.epa.gov/ghgemissions/global-greenhouse-gas-emissions-data>).

Simulation Study of the Integration of Hydrogen Fuel Cells into Unmanned Aerial Vehicles (UAV) and Estimation of the Emission Savings Achieved when Compared to a UAV with a Gasoline Combustion Engine



UNIVERSITAT
POLITÈCNICA
DE VALÈNCIA



ESCUELA TÉCNICA
SUPERIOR INGENIEROS
INDUSTRIALES VALENCIA

BUDGET

SIMULATION STUDY OF THE INTEGRATION OF HYDROGEN FUEL CELLS INTO UNMANNED AERIAL VEHICLES (UAV) AND ESTIMATION OF THE EMISSION SAVINGS ACHIEVED WHEN COMPARED TO A UAV WITH A COMBUSTION ENGINE

BUDEGT INDEX

1 SCOPE.....	1
2 PERSONNEL COSTS.....	2
3 COMPUTER EQUIPMENT AND SIMULATION SOFTWARE.....	4
4 MATERIAL EXECUTION BUDGET.....	5
5 CONTRACT EXECUTION BUDGET.....	6
6 BIDDING BASE BUDGET.....	7

1 SCOPE

The Master's Project Budget aims to estimate the economical value of the work carried out for the design and comparison of two hybrid electric systems power sources for unmanned aerial vehicles.

Firstly, the personnel expenses will be included according to the criteria provided by the R&D&I Management Service of the Polytechnic University of Valencia (SGI-UPV) based on an hourly dedication and salary compensation. In addition, an estimation of the computer equipment used and the cost of the simulation software license will be included.

The Budget does not include the costs for the commercial materials or the manufacture of the drone systems, nor the electronic equipment which makes up the drone flight systems (control elements, cameras...).

As the flights carried out were done by an external company and before the project commencement, these costs have also been excluded from the budget.

2 PERSONNEL COSTS

The details of costs associated with the expenditure of those who carried out research for purpose of the project according to time dedication will be outlined here.

To establish the salary of personnel who contributed to the project, the suggestions provided by the university were utilised. These personnel included Iona McNair as a recently graduated Chemical & Process Engineer, in addition the addition of Alvaro Montero and Carlos Sanchez as Research Teaching Staff (PDI) shall be incorporated with thanks for their contributions. In accordance with the Recommendations on the Preparation of Budgets in R&D&I Activities, the hourly cost of personnel is defined by following the below tables of the SGI-UPV.

CATEGORIA PLANTILLA UPV	CATEGORÍA EN LA ACTIVIDAD	Horas/año facturables ²	Coste directo por hora ²
Catedrático/a de Universidad	Responsable	1.650	55,5
Titular de Universidad	Experto	1.650	41,3
Prof. Contratado Doctor		1.650	38,1
Ayudante Doctor	Técnico	1.650	20,9
Ayudante		1.650	18,3
Catedrático/a de Escuela Universitaria		1.650	41,5
Titular de Escuela Universitaria		1.650	31,6
Profesor Colaborador		1.650	38,5

CATEGORIA	Retribución anual bruta		Coste anual con S.S. (32,1%) e indemnización (3,04%)		Coste horario (Incluido S.S.)	
	Min	Máx	Min	Máx	Min	Máx
Doctor contratado	16.849,84	40.956,86	22.770,87	55.349,10	12,94	31,45
FPI Años 1 y 2	16.849,84	32.540,48	22.770,87	43.975,20	12,94	24,99
Titulado superior	16.849,84	32.540,48	22.770,87	43.975,20	12,94	24,99
Titulado medio	14.569,66	26.032,44	19.689,44	35.180,24	11,19	19,99
Especialista técnico	C16:	C19:	C16:	C19:	C16:	C19:
	20.396,60	21.846,58	27.563,97	29.523,47	15,66	16,77

Alvaro Montero and Carlos Sanchez are estimated to receive a salary of €41.30/h as both belong to the University Professor category as highlighted above. The salary of Iona McNair is set at €20/h, which represents the average salary between the minimum and maximum corresponding to a Higher Degree category. The hours were calculated by consider a 10-hour day 5 days a week for the duration of the 12 weeks for Iona McNair, and took into consideration the meetings and research time carried out by University Professors.

Simulation Study of the Integration of Hydrogen Fuel Cells into Unmanned Aerial Vehicles (UAV) and Estimation of the Emission Savings Achieved when Compared to a UAV with a Gasoline Combustion Engine

Code	Personnel	Title	Time (hours)	Price (€)	Subtotal (€)	Total (€)
1.1	Iona McNair	Higher Degree	600	20	12,000	
1.2	Alvaro Montero	University Professor	30	41.3	1,239	
1.3	Carlos Sanchez	University Professor	10	41.3	413	13,652

3 COMPUTER EQUIPMENT AND SIMULATION SOFTWARE

The details of costs related to the computer equipment and simulation software license will be displayed here.

According to the Recommendations on the Preparation of Budgets in R&D&I Activities (SGI-UPV), the computer equipment and simulation software costs can be estimated from the following equation:

$$Cost (\text{€}) = Use (\text{years}) \cdot \frac{Price (\text{€})}{Amortization Period (\text{years})}$$

Clasificación económica del gasto		Amortización (años)
68358	Adquisición de equipos para procesos de información	6
68359	Adquisición de aplicaciones informáticas	6
68360	Adquisición de maquinaria	12
68361	Adquisición de instalaciones técnicas	12
68362	Adquisición de útiles y herramientas	12
68363	Adquisición de otro inmovilizado material	12
68364	Adquisición de equipos didácticos y de investigación	10

The laptop used was the Lenovo Yoga 520 model with an approximate market price of €599 and an estimated lifetime of 6 years. The laptop was used for the writing of the memory, alongside the analysis of data provided by the simulation, for which it presents a complete use equivalent to the entire duration of this Master's Final Project (~12 weeks).

The purchase of the TRNSYS18 simulation software license for educational use represents a cost of €2,250 for a 10 unit batch, meaning an equivalent unit price of €225 for the period required. Despite the simulation being carried out prior to this project commencing, the simulation software was essential to the project. Therefore, the use was partial with respect to the duration of the project (~2 weeks).

Code	Item	Measurement	Price (€)	Subtotal (€)	Total (€)
2.1	Lenovo Yoga 520 Laptop	1	25	25	
2.2	Software (TRNSYS 18)	1	2.2	2.2	27.2

4 MATERIAL EXECUTION BUDGET

This adds together the costs associated with the partial budgets mentioned previously, named Material Execution Budget (PEM):

Material Execution Budget (PEM)	Cost (€)
No. 1. Personnel Expenses	13,652
No. 2. Computer Equipment and Simulation Software	27.2
TOTAL	13,679.2

The Material Execution Budget (PEM) amounts to THIRTEEN THOUSAND SIX HUNDRED AND SEVENTY NINE EUROS AND TWENTY CENTS

5 CONTRACT EXECUTION BUDGET

The Contract Execution Budget (PEC) is obtained by the addition of the General Expenses as Indirect Costs (GG) estimated as 25% of the Material Execution Budget (PEM). This relates to the electrical consumption of computer equipment and the cost of rental offices of the university staff and degree holders.

The Industrial Benefit (BI) of 6% of the Material Execution Budget is also applied for when trying to commercially invoice the project.

Contract Execution Budget (PEC)	Cost (€)
Material Execution Budget (PEM)	13679.2
General Expenses (GG) 25%	3419.8
Industrial Benefit (BI) 6%	820.75
TOTAL	17919.75

The Contract Execution Budget (PEC) amounts to SEVENTEEN THOUSAND NINE HUNDRED AND NINETEEN EUROS AND SEVENTY FIVE CENTS

6 BIDDING BASE BUDGET

This incorporates the 21% VAT on the Contract Execution Budget (PEC):

Bid Base Budget (PBL)	Cost
Contract Execution Budget (PEC)	17,919.75
VAT 21%	3,763.15
TOTAL	21,682.9

The Bid Base Budget (PBL) amounts to TWENTY ONE THOUSAND SIX HUNDRED AND EIGHTY TWO EUROS AND NINE CENTS



UNIVERSITAT
POLITÈCNICA
DE VALÈNCIA



ESCUELA TÉCNICA
SUPERIOR INGENIEROS
INDUSTRIALES VALENCIA

APPENDICES

SIMULATION STUDY OF THE INTEGRATION OF HYDROGEN FUEL CELLS INTO UNMANNED AERIAL VEHICLES (UAV) AND ESTIMATION OF THE EMISSION SAVINGS ACHIEVED WHEN COMPARED TO A UAV WITH A COMBUSTION ENGINE

INDEX OF APPENDICES

A-1. PEMFC COMPONENTS.....	1
A-2. FIRST & SECOND LAW OF THERMODYNAMICS.....	4
A-3. IMPACT OF TEMPERATURE.....	5
A-4. IMPACT OF PRESSURE.....	6
A-5. HALF-CELL REACTION MECHANISMS.....	7
A-6. EXPENDED ENERGY OF COMBUSTION ENGINE-BATTERY HYBRID.....	9
A-7. SIMPLISTIC THEORETICAL FUEL CELL EFFICIENCY.....	11
A-8. THERMODYNAMIC POTENTIAL OF A THEORETICAL FUEL CELL.....	13
A-9. DESCRIPTION OF DRONE FLIGHT PHASES.....	15
A-10. QUATERNIUM DATA.....	16

A-1. PEMFC COMPONENTS

A-1.1 Proton Exchange Membrane (Electrolyte)

The major difference which lies between different fuel cell configurations is the nature of the electrolyte solution. In the case of a PEMFC, a polymer cation exchange membrane is used as a solid sheet of electrolyte which performs several critical functions to ensure correct operation of the system.

The electrolyte presents a physical barrier between the anodic and cathodic components, meaning there is a low reactant 'cross-over'. This results in direct contact between the fuel and oxidising agent being prevented. However, the electrolyte must allow passage of protons from the anodic region to the cathodic region in order to complete the electrochemical half-cell reactions, and thus must present high ionic conductivity. The electrolyte must prevent the movement of electrons through the medium of the electrolyte to force the electronic path through the conductive element of the fuel cell which connects both the electrodes, and thus generating an external electrical current (Je Seung Lee and Dinh Quan 2005).

The polymeric membrane must have high ionic conductivity to guarantee the transport of ions through the electrolyte. A mechanism named Grotthuss (or proton jumping) is followed for the process of ion transport in the electrolyte medium. Here, a proton hopping mechanism occurs on water molecules which are held within the polymeric structure of the membrane. To achieve maximum ionic conductivity, the polymeric membrane of the electrolyte must be kept hydrated, using the water produced via the reduction of oxygen where necessary for wetting (Anon n.d.).

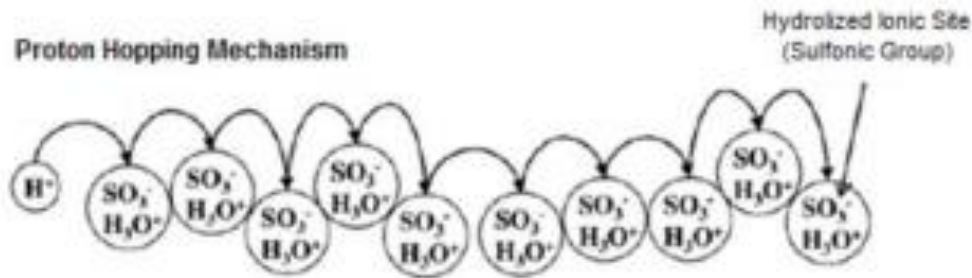


Figure 16- Grotthuss proton hopping mechanism (31)

A-1.2 Bipolar Plates

The bipolar plates are located at the ends of the fuel cell and are responsible for enabling the diffusion of reactive gases on the catalytic surface of the electrodes. In addition, they conduct electrical current away from the gas diffusion layer of the fuel cell, as the current is conducted from the positive electrode of one cell to the negative electrode of the next. This conduction gives them the role of current collectors as they allow a series connection of various electrochemical single cells to achieve the final configuration of the cell.

The materials of construction for bipolar plates should be lightweight but strong, have good electrical conductivity but low ionic conductivity, and be impermeable to reactive gases. The most commonly used material is graphite (autam n.d.), however there are also other models under development using stainless steel and aluminium alloys.

A bipolar plate features a diffusion channel design in which the direction, size and depth for the reactive gases is critical to achieving a homogeneous distribution of fuel and oxidising agent on the catalyst surface

of the electrodes. It must also allow the escape of water vapour generated in the cathodic region and, as far as possible, avoid the development of liquid water inside the channels as this could hinder the distribution of reactive gases (Isanaka et al. 2012).

To achieve a homogeneous distribution of reactive gases on the catalytic surface of the electrodes, varying sizes and shapes of bipolar plates are used. There are numerous designs for bipolar plates, with the serpentine and parallel configurations represented in *Figure 17*. These have shown great effectiveness in the uniform diffusion process of the reactive gases.

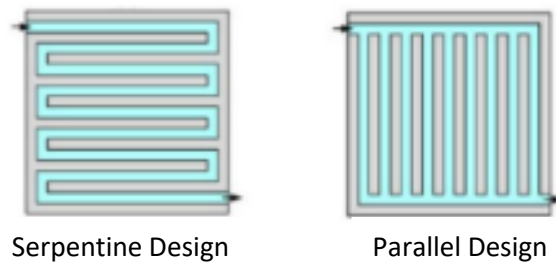


Figure 17- Bipolar plates configurations

A-1.3 Gas Diffusion Layer

Situated between the bipolar plate and the electrocatalyst, this layer (often referred to as GDL) conducts electrons between the bipolar plate and the electrocatalyst. Due to the channels present in the bipolar plates, the GDL facilitates the diffusion of the reactive gases over the entire surface of the electrodes. The gas diffusion layer also helps to aid water management through the use of hydrophobic polymers (UNGAN and BAYRAKÇEKEN YURTCAN 2020).

A-1.4 Catalyst and Electrodes

In the case of PEM-type fuel cells, the 'anode/electrolyte/cathode' configuration represents the central unit of a single fuel cell and is designated as the membrane electrodes (Membrane Electrode Assembly, MEA).

When using a polymeric material as a solid electrolyte, certain temperature conditions must be met to guarantee the structural integrity of the exchange membrane. The most common operating temperature for a PEMFC is approx. 80°C. This results in a slower electrochemical half-reaction pace, especially the oxygen reduction half-reaction where the kinetics are much more sluggish. The role of the catalyst is therefore essential to increase the kinetics of the electrochemical half-reactions (Salam et al. 2020). (Litster and Mclean 2004)

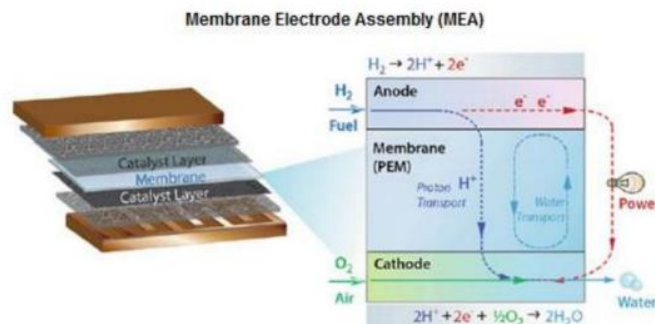


Figure 18- Structure of membrane electrodes (36)

The active surface of the catalytic sheets present in the MEA is obtained by the accumulation of platinum particles supported on a porous carbon environment. By taking advantage of the platinum dispersion process on carbon support particles it is possible to maximise the surface area of the electrocatalyst to increase the catalytic activity in electrochemical half-reactions (Li et al. 2022).

A-2. FIRST & SECOND LAW OF THERMODYNAMICS

The first law of thermodynamics, also known as the law of conservation of energy, states that any change in the energy of a system must be fully accounted for by energy transfer in the surroundings. The two ways in which energy can be transferred between a closed system and the surrounding is through heat (q) and work (w).

$$d(\text{Energy})_{univ} = d(\text{Energy})_{system} + d(\text{Energy})_{surroundings} = 0 \quad \text{Equation A-2.1}$$

$$dU = \delta q - \delta w \quad \text{Equation A-2.2}$$

As only the mechanical expansion work exerted by the system against the pressure (p) is considered, the electrical work performed by the fuel cell to generate electricity can be disregarded.

$$dU = dq - p.dV \quad \text{Equation A-2.3}$$

The second law of thermodynamics introduces the concept of entropy, a thermodynamic quantity representing the unavailability of a systems thermal energy for conversion into mechanical work. Except in the case of extremely simple systems, it is impossible to determine exactly the value of entropy in a system. Entropy (S) is therefore determined from the reversible heat transfer (Q_{rev}) under constant pressure and temperature (T) conditions.

$$dS = \frac{\delta Q_{rev}}{T} \quad \text{Equation A-2.4}$$

By combining the expressions for the first and second laws allows the internal energy variation of the system to be expressed from the independent variables within the system including the entropy changes and volume (V).

$$dU = TdS - p.dV \quad \text{Equation A-2.5}$$

A-3. IMPACT OF TEMPERATURE

A temperature variation at constant Gibbs free energy expression can be used to understand the effect of operating temperature on the electrode potential where pressure is constant.

$$dG = -S \cdot dT + V \cdot dp \Rightarrow \left. \frac{dG}{dT} \right|_{p = \text{cnst}} = -S \quad \text{Equation A-3.1}$$

As the relationship between the Gibbs free energy and electrode potential has already been defined, an expression of the electrode potential as a function of temperature can be defined.

$$\Delta G = -n \cdot F \cdot E \Rightarrow \left. \frac{dE}{dT} \right|_{p = \text{cnst}} = \frac{\Delta S}{n \cdot F} \quad \text{Equation A-3.2}$$

As the electrode potential can be defined at an arbitrary temperature (E_T), the parameter can be calculated -by setting a reference temperature the same as that under standard conditions. The electrode potential is then found from the reversible electrode potential (E^0).

$$E_T = E^0 + \frac{\Delta S^0}{n \cdot F} \cdot (T - T_0) \quad \text{Equation A-3.3}$$

As shown in the above equation, the entropy variation of the global reaction represents the parameter that marks the relationship between the electrode potential of a fuel cell and temperature. As the absolute temperature is always positive, the dependence of the fuel cell efficiency varies with temperature according to the sign of the entropy. For a polymer electrolyte membrane fuel cell, the entropy change for the electrochemical oxidation reaction of hydrogen under standard conditions has a negative sign ($\Delta S^0 < 0$), indicating that the electrode potential decreases with increasing operating temperature. This temperature influence is shown in *Figure 19*.

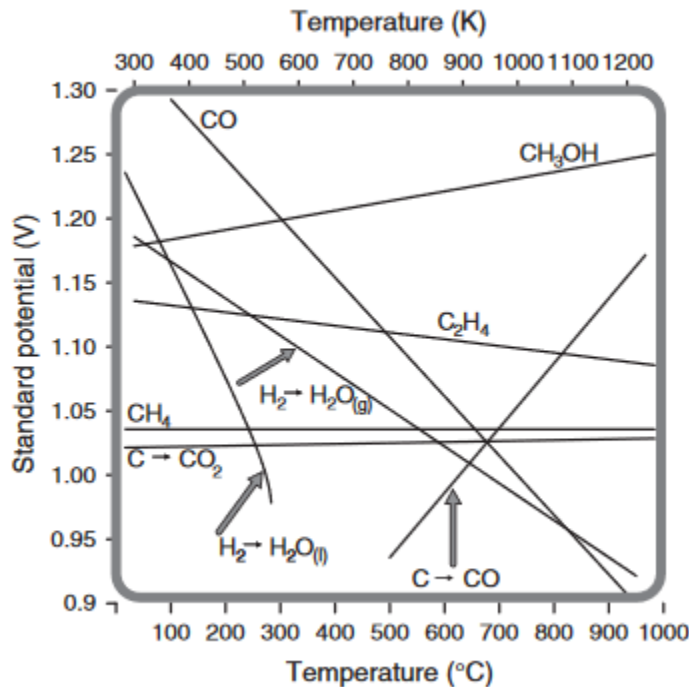


Figure 19- Influence of temperature on electrode potential (38)

A-4. IMPACT OF PRESSURE

Similar to temperature, pressure has an impact on the electrode potential. To understand this effect, a pressure variation at constant temperature is considered for the Gibbs free energy expression.

$$dG = -S \cdot dT + V \cdot dp \Rightarrow \left. \frac{dG}{dp} \right|_{T = \text{cnst}} = V \quad \text{Equation A-4.1}$$

By applying the relationship between the Gibbs free energy and electrode potential, an expression of the electrode potential as a function of pressure can be achieved.

$$\Delta G = -n \cdot F \cdot E \Rightarrow \left. \frac{dE}{dp} \right|_{T = \text{cnst}} = -\frac{\Delta V}{n F} \quad \text{Equation A-4.2}$$

Therefore, it is shown that the variation of the reversible cell voltage with pressure is related to the volume change of the reaction. If the volume change of the reaction is negative (for instance, fewer moles of gas are generated by the reaction than consumed), then the cell voltage will increase with increasing pressure. This is an example of *Le Chatelier's principle*, where increasing the pressure of the system favours the direction that relieves the stress applied to the system.

Considering the chemical substances within the gas phase which usually produce a significant volume change, and by assuming the ideal gas law applies, a relationship between the variation of electrode and operating pressure can be estimated.

$$\left. \frac{dE}{dp} \right|_{T = \text{cnst}} = -\frac{(n_P - n_R) \cdot R \cdot T}{n \cdot F \cdot p} = -\frac{\Delta n_G \cdot R \cdot T}{n \cdot F \cdot p} \quad \text{Equation A-4.3}$$

Where Δn_G represents the change in the total number of moles of gas upon reaction. Since the variation in the global moles of gaseous species has a negative sign ($\Delta n_G < 0$), an increase in the operating pressure provides a higher electrode potential for the PEMFC (O'Hayre et al. 2016).

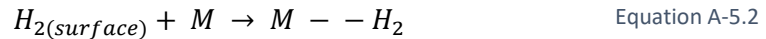
A-5. HALF-CELL REACTION MECHANISMS

The reaction mechanism for HOR is fairly simple, involving five stages in the following sequence:

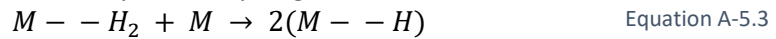
- 1) Mass transport of H₂ to the electrode



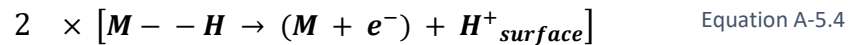
- 2) Adsorption of H₂ to surface



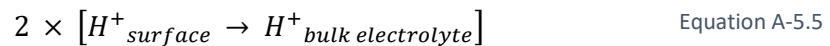
- 3) Separation of H₂ molecule to individually bound hydrogen atoms



- 4) Transfer of electrons from H to H⁺



- 5) Mass transfer of H⁺ away from the electrode



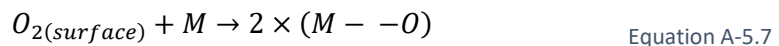
The rate of the overall reaction is limited by the kinetics of the slowest step in the proposed reaction mechanism, named the rate determining step. In the case of the hydrogen oxidation reaction, the electron transfer between the hydrogen atom adsorbed on the electrode surface represents the limiting step.

The steps which make up the direct 4-electron dissociative mechanism for the cathodic reaction are similar to that for the anodic reaction presented previously.

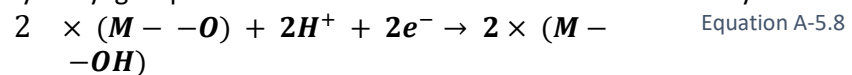
- 1) Mass transport of O₂ to the electrode



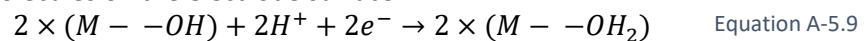
- 2) Absorption of O₂ to the surface and the dissociation of O atoms



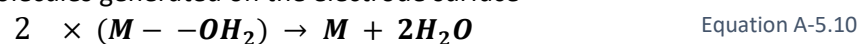
- 3) Formation of adsorbed hydroxyl groups on the interface of the electrode and electrolyte



- 6) Formation of water molecules on the electrode surface



- 7) Desorption of water molecules generated on the electrode surface



The rate limiting step for the mechanism displayed above is the fourth step where the electrochemical reduction of adsorbed hydroxyl groups are used to form water molecules on the surface of the cathode electrode.

A-6. EXPENDED ENERGY OF COMBUSTION ENGINE-BATTERY HYBRID

Drones expend energy to fight gravity and counter drag forces due to forward motion and wind. To be able to determine this expended power, some parameters must be known. The speed and weight must be known, for the purpose of this calculation a range of values were analysed. Firstly, the thrust necessary for the drone to stay airborne and travel forwards at the desired velocity was determined. It was assumed that the thrust from each rotor is roughly equal and when combined exactly balance gravity and drag forces. The total thrust required was found by:

$$TH = m_{total} * g + F_{drag} \quad \text{Equation A-6.1}$$

Similarly, assuming that the flight is steady, the pitch angle can be calculated though:

$$a = \tan^{-1} \left(\frac{F_{drag}}{m_{total} * g} \right) \quad \text{Equation A-6.2}$$

The drag force necessary for these calculations is estimated using the following:

$$F_{drag} = \frac{1}{2} \rho v^2 C_D A \quad \text{Equation A-6.3}$$

The drag coefficient, C_D , is required for the drag force calculation. However, it is difficult to determine this accurately due to the multiple sources of drag and so estimations were made based on various sources. The effective drag coefficient varies with velocity, where higher drag coefficients are found at higher velocities. The drag coefficient was estimated from a best-fit value of 1.2 for higher velocities and 0.8 for stationary flight velocity (Hwang, Cha, and Jung 2018; Polivanov and Sidorenko 2021; Stolaroff et al. 2018). These values were applied using interpolation of the different sizing/weights/velocities depending on the measurement variable given for the source.

With the thrust it is possible to calculate the power requirement for a steady flight. The theoretical minimum power is dependent on the area swept by the rotors. For the theoretical minimum power calculation, the following equation can be applied:

$$P_{min,hover} = \frac{TH^{3/2}}{\sqrt{\frac{1}{2} \pi n D_b^2 \rho}} \quad \text{Equation A-6.4}$$

When the drone moves at a significant velocity or in a substantial wind, the minimum power requirement changes depending on the speed and pitch angle. This minimum power requirement is given by:

$$P_{min} = TH(vs \sin \alpha + v_i) \quad \text{Equation A-6.5}$$

Here, v_i is the induced velocity required for the given thrust requirement and is found using the following equation:

$$v_i = \frac{2TH}{\pi n D^2 \rho \sqrt{(v \cos \alpha)^2 + (vs \sin \alpha + v)^2}} \quad \text{Equation A-6.6}$$

The expended power can then be calculated using the minimum power and overall power efficiency of the drone:

$$P = \frac{P_{min}}{\eta}$$

Equation A-6.7

A-7. SIMPLISTIC THEORETICAL FUEL CELL EFFICIENCY

By considering the enthalpy of formation under standard conditions ($p = 1 \text{ bar}$; $T = 25^\circ\text{C} = 298.15\text{K}$) shown in the table below for the chemical species involved in the electrochemical oxidation reaction of hydrogen, the maximum energy that can be produced from the hydrogen fuel in a PEMFC is calculated (Chase 1998).

Table 9- Enthalpy of formation under standard conditions for electrochemical oxidation reaction

Chemical Species	$H_F^\circ (\text{kJ/mol})$
Liquid water, H ₂ O (l)	-285.83
Hydrogen, H ₂ (g)	0
Oxygen, O ₂ (g)	0

$$\begin{aligned} \Delta H^0 &= Q_{max}^\circ = \text{products} - \text{reactants} \\ &= (H_F^0)_{H_2O} - (H_F^0)_{H_2} - \frac{1}{2} \cdot (H_F^0)_{O_2} = -285.83 \frac{\text{kJ}}{\text{mol H}_2} \end{aligned} \quad \text{Equation A-7.1}$$

Therefore, the electrochemical oxidation of hydrogen fuel releases around 286 kJ/mol of H₂, making it an exothermic reaction. However, relating back to the second law of thermodynamics, any process that involves heat transfer results in a change in the entropy of the system, thus the amount of energy which can be converted into electricity is limited.

The total amount of energy stored in the hydrogen fuel that can be used to generate electricity by performing useful work should be calculated. The value relates to the change in Gibbs free energy of the system and can be termed work potential.

This work potential can be determined by utilising the expression for Gibbs free energy. Having the values for just enthalpy and entropy it is possible to calculate the work potential of a PEMFC.

$$dG = dH - TdS \quad \text{Equation A-7.2}$$

$$\Delta G = [(H_F)_{prod} - (H_F)_{reac}] - T \cdot [(S_F)_{prod} - (S_F)_{reac}] \quad \text{Equation A-7.3}$$

By considering the entropy values of the chemical species involved in the global chemical reaction of hydrogen under standard conditions ($p = 1 \text{ bar}$; $T = 25^\circ\text{C} = 298.15\text{K}$) shown in the table below, the work potential can be obtained (Anon 2016).

Table 10- Entropy values for electrochemical oxidation reaction

Chemical Species	$S_F^0 (\text{J/mol.K})$
Liquid water, H ₂ O (l)	69.9
Hydrogen, H ₂ (g)	131
Oxygen, O ₂ (g)	205

$$\Delta S^0 = (S_F^0)_{H_2O} - (S_F^0)_{H_2} - \frac{1}{2} \cdot (S_F^0)_{O_2} = -163.6 \frac{\text{J}}{\text{mol H}_2 \cdot \text{K}} \quad \text{Equation A-7.4}$$

$$\Delta G^0 = \Delta H^0 - T_0 \cdot \Delta S^0$$
$$= -285.83 \left(\frac{\text{kJ}}{\text{mol H}_2} \right) - 298.15(\text{K}) \cdot - \frac{163.6}{1000} \left(\frac{\text{kJ}}{\text{mol H}_2 \cdot \text{K}} \right) \quad \text{Equation A-7.5}$$

$$\Delta G^0 = -237.053 \frac{\text{kJ}}{\text{mol H}_2} \approx -237 \frac{\text{kJ}}{\text{mol H}_2} \quad \text{Equation A-7.6}$$

From the results obtained using standard conditions, it is demonstrated that there is a large percentage of the calorific power of the hydrogen fuel ($237.053/285.83 = 82.93\%$) is able to produce electrical work. The remaining 48.8 kJ/mol of H₂ is irreversibly lost as heat to the environment. As the Gibbs free energy (ΔG) is less than zero, the electrochemical oxidation of hydrogen is a spontaneous reaction which is energetically favourable and so there is no requirement for external energy.

A-8. THERMODYNAMIC POTENTIAL OF A THEORETICAL FUEL CELL

The thermodynamic potential is obtained by the Nernst equation whilst taking the effect operating temperature and the pressure of reactive gases into consideration. Therefore, the following equation can be developed:

$$E = E^0 + \frac{\Delta S^0}{n \cdot F} \cdot (T - T_0) + \frac{R \cdot T}{n \cdot F} \cdot \ln(p_{H_2} \cdot p_{O_2}^{1/2}) \quad \text{Equation A-8.1}$$

$$E = 1.23 - 0.00085 \cdot (T_{stack} - 298) + 0.0000431 \cdot T_{stack} \cdot \ln(p_{H_2} \cdot p_{O_2}^{1/2}) \quad \text{Equation A-8.2}$$

The voltage losses due to activation polarisation (η_{act}) are developed from the Bulmer- Volmer expression which establishes a relationship between the current density generated and the overpotential obtained.

$$i = i_0 \cdot \left[e^{\frac{\alpha \cdot \eta \cdot F \cdot n}{R \cdot T}} - e^{\frac{-(1-\alpha) \cdot \eta \cdot F \cdot n}{R \cdot T}} \right] \quad \text{Equation A-8.3}$$

According to research conducted by Amphlett's group where a semi-empirical formula for calculating voltage losses due to activation in a PEMFC was developed, there are 4 parameters to be considered. The overall expression is obtained as a function of the operating temperature, oxygen concentration in active centres of anodic electrode surface and the current density generated by electrochemical system.

$$\eta_{act\ total} = \eta_{act\ anodic} + \eta_{act\ cathodic} = \varepsilon_1 + \varepsilon_2 T + \varepsilon_3 T (\ln[C_{O_2}]) + \varepsilon_4 T (\ln[i]) \quad \text{Equation A-8.4}$$

Where the constant parametric coefficients can be expressed as follows

$$\varepsilon_1 = \left(\frac{-\Delta F}{\alpha n F} \right) + \left(\frac{-\Delta F}{2 F} \right) \quad \text{Equation A-8.5}$$

$$\varepsilon_2 = \frac{R}{\alpha n F} \cdot \ln(n F A_e k^0 [C_H]^{1-\alpha} \cdot [C_{H_2O}]^\alpha) + \frac{R}{2 F} \ln(4 F A_e k^0 [C_{H_2}]) \quad \text{Equation A-8.6}$$

$$\varepsilon_3 = \frac{R}{\alpha n F} (1 - \alpha) \quad \text{Equation A-8.7}$$

$$\varepsilon_4 = - \left(\frac{R}{\alpha n F} + \frac{R}{2 F} \right) \quad \text{Equation A-8.8}$$

Applying this overall activation polarisation expression with the parametric coefficients allows for the following equation to be obtained:

$$\eta_{act} = -0.95 + 0.00243 \cdot T_{stack} + 0.000076 \cdot T_{stack} \cdot \ln[C_{O_2}] - 0.000192 \cdot T_{stack} \cdot \ln \left[\frac{I_{FC}}{A_{PEM}} \right] \quad \text{Equation A-8.9}$$

Voltage losses in the ohmic region can be modelled neglecting the contribution of resistance of the external circuit and electrode passage of electric current on internal resistance, which results in the following equation:

$$\eta_{ohmic} = IR = I \cdot (R_{elec} \cdot R_{ion}) = IR_{ion} \quad \text{Equation A-8.10}$$

Ohmic losses occur due to the resistance to the passage of ionic charge through the electrolyte medium. This is equivalent to considering just the ionic resistance presented by the fuel cell (η_{ohmic}) and thus

depends heavily on the degree of wetting in the membrane (γ), as the diffusion of protons from the anodic region to the cathodic region is facilitated according to the Grotthuss mechanism.

By considering the interaction and quadratic effect of current density ($i_{FC} = I_{FC}/A_{PEM}$) and the operating temperature (T_{stack}) on the internal resistance of the fuel cell. However, consideration should be taken for the thickness of the membrane (t_{PEM}) and wetting condition of the membrane, which arrives at the following empirical expression.

$$\eta_{ohmic} = \frac{I_{FC} \cdot t_{PEM}}{A_{PEM}} \cdot \frac{8}{\exp\left(3.6 \left[\frac{T_{stack} - 353}{T_{stack}}\right]\right)} \cdot \left(1 + 1.64 \cdot \frac{I_{FC}}{A_{PEM}} + \gamma \left[\frac{I_{FC}}{A_{PEM}}\right]^3\right) \quad \text{Equation A-8.11}$$

The output voltage of the PEMFC fuel cell (U_{stack}) can be obtained once the voltage provided by a single fuel cell is known from the number of cells connected in series:

$$U_{stack} = N_{cells} \cdot U_{cell} \quad \text{Equation A-8.12}$$

A-9. DESCRIPTION OF DRONE FLIGHT PHASES

The start phase:

To turn on the drone's flight systems (navigation systems, communication...) and start powering the balance of the system requires the start-up of the power source, with the LiPo battery beginning to provide all the necessary current intensity for a time period of approximately 1 minute.

Take-off phase:

Until the primary power source, either the fuel cell of the ICE-EG, is operational, the aircraft cannot begin to climb. Therefore, in the moments before taking off from the ground, the intensity of the current demanded by the drone increases progressively linearly for 1 minute before reaching the maximum consumption peak which marks the beginning of the drone ascent. To guarantee safe ascent until reaching sufficient flight altitude, a period of time of 3 minutes was established where the maximum consumption of electrical current by the drone was sustained.

As long as the current intensity generated by the fuel cell is capable of fully supplying the total demand of the drone and covers the energy requirement of the balance of the system, the battery is not required during the take-off phase. However, the total demand of the drone is greater than that of the electrical current generated by the power source, the LiPo battery provides the additional demand of the drone.

Stationary flight phase:

When the drones upward path reaches a sufficient flight altitude, a stationary flight phase begins, characterised mostly by horizontal displacement. In relation to the total flight path, the plane flight phase is the one which lasts the longest and where the greatest fuel consumption occurs. During the horizontal trajectory the stable energy demand which is established is lower than that of the maximum consumption peaks in the take-off and landing phases.

It was established that a stationary flight phase of 50 minutes would be adequate.

Landing phase:

When the drone has completed the horizontal displacement in the stationary phase to reach the action area of the level of the fuel in the tank is too low and insufficient the descending path begins. To guarantee safe descent to the ground, the landing begins with a period of time of 2-3 minutes where the maximum consumption peak of the drone is maintained. In the final moments of landing on the ground, the current intensity demanded by the drone decreases progressively linearly for 1 minute, starting at the maximum consumption peak and dropping until the plant balance demand that marks the end of the drones landing is reached. It can be considered that the operating principle of the hybrid system in the take-off and landing phases are practically equivalent.

Stop phase:

To stop the drone flight systems and the plant balance, the LiPo battery stops being in operation and the power source itself begins to progressively decrease the electrical current for 1 minute approximately.

A-10. QUATERNIUM DATA

Table 11 illustrates the data received from *Quaternium* following the site visit. This data proved to be vital in the development and progress of the project.

Table 11- Hybrix 2.1 data provided by Quaternium

Weight in Flight (kg)	Required Electrical Power (W)	Approx. Fuel Consumption (L/h)
24	2600	2.3
17.5	1600	1.2
13	960	0.7